The processes responsible for the epigenetic changes that lead to dedifferentiation are referred to as nuclear reprogramming mechanisms (Rideout *et al.*, 2001). Nuclear reprogramming in this sense refers to the process by which a specialized nucleus re-acquires developmental capacity. This definition includes complete reprogramming to a totipotent state (verifiable only by generation of viable offspring) and also partial reprogramming where pluripotency (the capacity to generate cells representative of all three germ layers) is restored. By necessity, it involves heritable changes to gene expression, i.e. changes in gene expression that are passed on to daughter cells. Some have suggested that transient changes to gene expression constitute nuclear reprogramming (Hakelien *et al.*, 2002), but such changes do not persist, nor is there any evidence that they are transferred to progeny cells. Such observations almost certainly result from residual transcription activity rather than the consequence of a reprogrammed genome, and so these examples do not constitute nuclear reprogramming as defined here and elsewhere (Hochedlinger and Jaenisch, 2006).

Naturally induced nuclear reprogramming

The differentiated state of cells is found to be extremely stable (Kato and Gurdon, 1993). The only stage during which normal mammalian cells seem to naturally dedifferentiate immediately follows fertilization (Schultz *et al.*, 1999). The sperm and oocyte, both highly differentiated cells with condensed chromatin structure, fuse to produce a zygote. Within the zygote, changes lead to the reversion to a less specialised totipotent cellular state (Kelly, 1977). Although the mechanism responsible is unknown, two events are associated with this dedifferentiation: chromatin structure becomes less dense: protamines are removed from sperm-derived chromatin and replaced by oocyte-derived histones (Perreault, 1992); and methylated haploid parental genomes are demethylated (Barton *et al.*, 2001).

Additionally, it has been speculated that inappropriate or incomplete nuclear reprogramming may occur in a pathological context, i.e. during the generation of teratomas. Teratomas are benign tumours associated with chaotic cell-lineage formation. The 'dedifferentiation' theory of cancer states that such lineages may arise from cells that have undergone dedifferentiation to a multipotent state (Ribbert, 1911). Teratomas can also be produced experimentally by injection of pluripotent stem cells into ectopic sites of a syngeneic animal (Evans and Kaufman, 1981; Matsui *et al.*, 1992; Rensnick *et al.*, 1992), so it is conceivable that inappropriately reprogrammed somatic cells could be the origin of such cancers.

Artificially induced nuclear reprogramming

In non-transformed somatic cells, once the differentiation programme of a cell has started, the process is normally irreversible. However, this programme may be reversed artificially. Using nuclear transfer (NT) (Wilmut *et al.*, 1997), cell fusion (Tada *et al.*, 1997), or even viral transduction of four specific stem cell genes (Takahashi and Yamanaka, 2006), it is possible to artificially and heritably alter a cell's gene expression and its functional identity. These techniques are collectively termed 'artificial induction of nuclear reprogramming' (**Figure 1**). The conversion of differentiated cells to pluripotent cells illustrates that cells do not permanently lose the ability to be pluripotent during differentiation.

Frustratingly, the mechanism by which a somatic nucleus may be reprogrammed remains unknown, aside from the fact that such a mechanism almost certainly involves both structural (Kikyo *et al.*, 2000) and chemical (Monk *et al.*, 1987) changes to chromatin. It may be possible for human somatic cells to be reprogrammed to a pluripotent state. If successful, this strategy would provide a potentially endless source of cells for biological research, as well as medical applications (Stojkovic *et al.*, 2005; Verlinsky *et al.*, 2005), toxicity assessment, drug testing and possibly even gene therapy (Wobus and Boheler, 2005). **Figure 2** illustrates how identification of reprogramming molecules and mechanisms could facilitate cell replacement therapy in humans. Over the past century, organ transplantation has evolved rapidly to the current widespread use of donated organs for the treatment of end-stage kidney, heart, and liver failure. However, with limited supplies of organs and an increasing demand for them, many patients who need transplants do not receive them (Gridelli and Remuzzi, 2000). The increasing gap between supply and demand for tissue and organ transplants means that harnessing nuclear reprogramming mechanisms is important (Sullivan and Eggan, 2007).

Nuclear transfer: the oldest and still the most reliable reprogramming technique

Spemann (1938) originally suggested transplantation of nuclei between cells as a technique to study the role of genetic material in cellular differentiation. In nuclear transfer, the nucleus from a differentiated donor cell is transplanted into an enucleated oocyte. The oocyte can reprogramme even an adult differentiated nucleus and the new cell can develop as an embryo. Artificially induced nuclear reprogramming by NT was first demonstrated by Briggs and King in 1952, when they showed that transfer of somatic nuclei to enucleated eggs can direct development so that tadpoles are generated (Briggs and King, 1952). Gurdon later refined the technique so that adult and fertile frogs could be generated (Gurdon *et al.* 1958). Decades later, the production of 'Dolly', the first viable mammal derived by reprogramming a fully differentiated adult somatic cell, illustrated that the mammalian nuclear genome can be completely reprogrammed and totipotency of the nucleus restored (Wilmut *et al.*, 1997). The nuclei of these offspring contain genomes of identical sequence to that of the nuclear donor. At present, nuclear transfer is the only technique in which one can accomplish total nuclear reprogramming in an unequivocal manner: by deriving viable offspring from a reconstituted embryo. More recently, embryonic stem (ES) cells have been derived from cloned mice (Wakayama *et al.*, 2001). The ES cells produced by somatic cell nuclear transfer retained self-renewal and pluripotent features, contributing to all germ layers, including the germline. In addition, gene expression profiling experiments showed the ES cell lines derived from cloned and fertilized mouse blastocysts are indistinguishable (Brambrink *et al.*, 2006). The NT–ES cells are developmentally and functionally equivalent to the fertilization-derived ES cells.

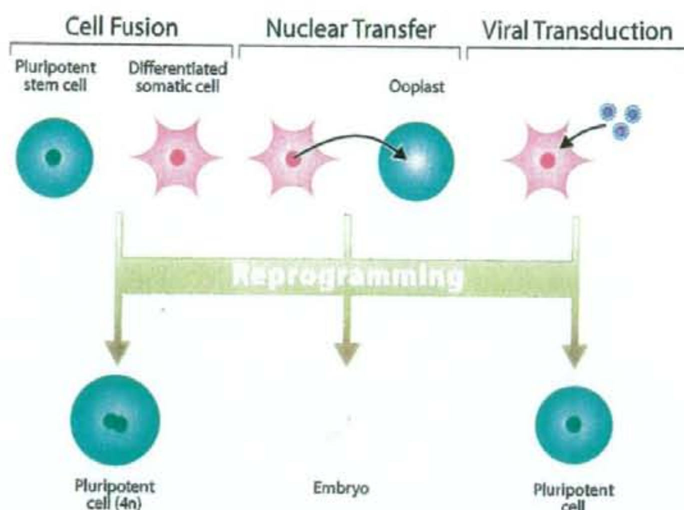

Figure 1. Artificially induced nuclear reprogramming. Cell fusion: a somatic cell fused with a pluripotent stem cell can be reprogrammed in the hybrid cell. These fused hybrid cells show similar features as embryonic stem (ES) cells; however the hybrid cell has a tetraploid karyotype and is unable to contribute to chimeras. Nuclear transfer: an adult somatic cell is transferred into an enucleated oocyte followed by artificial activation. These nuclear-transferred embryos can produce ES cells which are pluripotent, contributing to all germ layers including the germ cell lineage. Viral transduction: a somatic cell transduced by retroviruses expressing four key genes, *Oct3/4*, *Sox2*, *Klf4* and c-*Myc*, can be reprogrammed into iPS cells resembling ES cells in a cell-autonomous fashion. Only the nuclear transfer method can produce viable animals as it can return an adult nucleus to a totipotent, embryonic state.

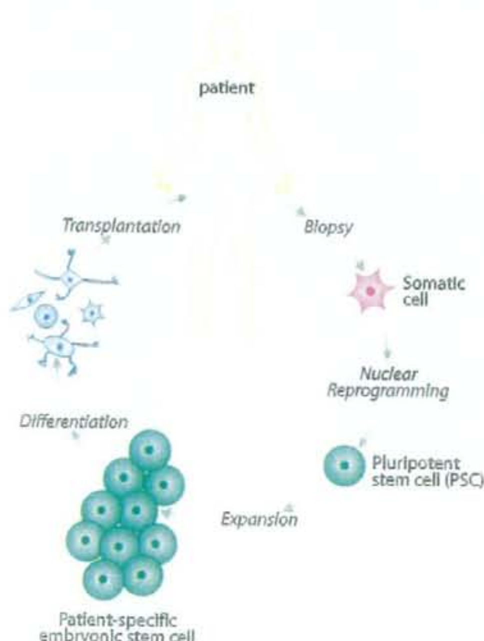

Figure 2. The ultimate goal of nuclear reprogramming research: controlled restoration of developmental potential. Once the mechanism by which nuclear reprogramming is understood, human somatic cells could be induced to dedifferentiate into pluripotent stem cells (PSC). PSC could then be expanded in culture and induced to redifferentiate into the cell type(s) required by the patient. These non-allogenic differentiated cells could then be transplanted into the patient with a decreased risk of immunorejection. It is also important to point out that patient matched pluripotent stem cells can also serve as in-vitro models for studying human disease and development at a cellular and molecular level. Such reprogramming will also allow the generation of genetically matched ES cells will, in themselves, provide scientists and clinicians an important new tool to recapitulate onset of specific diseases *in vitro* (Di Giorgio *et al.*, 2007).

Successful reprogramming of somatic nuclei by placing them in enucleated oocytes should perhaps not have been completely unexpected. There are compelling reasons why a system should exist for the removal of epigenetic modifications (excluding gametic imprints) in the oocytes and sperm. They are both highly specialized differentiated cells, and removal of their epigenetic patterns is essential to allow development of pluripotent cells from the inner cell mass (ICM). The same mechanism may be causing reprogramming of a somatic nucleus when exposed to the cytoplasm of an oocyte (Surani, 1999).

Many variables affect reprogramming success with NT. Some of these have been identified, i.e. structural integrity of the nuclear membrane (Willadsen 1986), quality and copy number of donor genetic material, chromatin conformation, histone composition, methylation and acetylation patterns (Campbell, 1999). Also important is the level of maturation or mitosis promoting factor (MPF) (Fulka *et al.*, 1996) and synchronization of donor and recipient cell cycles prior to embryo reconstruction (Campbell, 1996). High MPF concentrations in the oocyte and appropriate synchronization of donor and nuclear cell cycle using serum starvation are thought to minimize chromosomal damage and promote generation of reconstructed embryos that divide to produce normal diploid daughter cells.

Campbell suggests that the frequency of live offspring generation from reconstructed mammalian embryos made by NT is improved when the donor nuclei are in a quiescent state (Campbell *et al.*, 1996; Campbell, 1999). The successful production of Dolly, the first viable animal to be generated by nuclear transfer, used a nucleus from a cultured adult-differentiated somatic cell that had been serum starved into quiescence (Wilmut *et al.*, 1997). Kato *et al.* (1998) reported cloning of calves at 80% success ratio based on the number of transferred embryos using quiescent cumulus cells and oviduct epithelial cells that were cultured for several passages followed by serum starvation. Alternatively, using non-cultured cells also succeeded in producing cloned animals. Wakayama *et al.* (1998) used mouse cumulus cells, a naturally quiescent cell population, as nuclear donating cells in successful nuclear transfer experiments with mouse ooplasts. Ogura *et al.* (2000) made cloned mice by transferring Sertoli cells into enucleated mature oocytes. In both of these experiments, the cell cycle stage of the nuclear donors was controlled but the possibility that animals can be generated using non-quiescent cells as nuclear donors cannot be dismissed. Other researchers claim successful generation of mammalian offspring from nuclei not intentionally induced into a quiescent state (Cibelli *et al.*, 1998). Also, the possibility that transferred nuclei in Wakayama's and Ogura's experiments were non-quiescent cannot be eliminated.

Presumably, the importance of the state of the donor nucleus cell cycle is directly linked to compatibility with the recipient oocyte cytoplasm. Metaphase of second meiotic division (MII) oocytes has typically become the state of choice of recipient cytoplasts for NT procedures (Campbell *et al.*, 1996). MII oocytes contain active MPF to induce nuclear envelope breakdown (NEBD), premature chromosome condensation (PCC), and dispersion of nucleoli in the transferred nucleus, which may be essential for nuclear reprogramming. The donor nucleus in S phase of the cell cycle is likely to be incompatible with a high MPF state, leading to DNA damage and arrest at an early cleavage stage. However, inter-species NT experiments suggest that the occurrence and extent of NEBD and PCC in the donor nucleus are variable between different species, donor cell types and different procedures (Meissner and Jaenisch, 2006).

It had been thought previously that only the cytoplasm of the MII oocyte can support reprogramming after NT, so numerous species have been cloned by NT into MII oocyte (Meissner and Jaenisch, 2006). It seemed necessary for initiating reprogramming that the donor nucleus had elevated MPF concentrations, since NT embryos fail to develop, transforming into interphase zygotes (McGrath and Solter, 1984; Wakayama, 2000). However, more recently, a new insight disproving a myth of MII necessity for NT has been reported (Egli *et al.*, 2007). Unlike interphase zygotes, fertilized zygotes arrested in mitosis can fully support the reprogramming of somatic cells to the totipotent state. This indicates that factors sufficient for reprogramming are not limited to oocytes, and suggests that a continuum of activity extends beyond the unfertilized egg (Egli *et al.*, 2007). Why is the metaphase cell useful for reprogramming? A possible explanation is that condensed chromatin expels transcription factors like Oct-3/4 and Sox2 (Martinez-Balbas *et al.*, 1995), and without a nuclear membrane to enclose them, they are free to interact with any foreign chromatin introduced. Also, as the cell is poised to divide in M phase, it has synthesized many components of the cell to elevated levels, so presumably factors necessary for reprogramming are present in a greater abundance than at other stages of the cell cycle.

Experiments by Eggan *et al.* (2001) show that the number of live mice generated from cells reprogrammed via nuclear transfer is dependent on the genetics of the mouse from which the nuclear donor cell is taken. ES cells taken from inbred 129/SvJae mice fail to produce any post-natal surviving offspring, whereas cloned pups derived from ES cells of C57BL/6 and 129/SvJae matings can survive to adulthood. It may be that the use of inbred animals as nuclear donors introduces a reprogramming barrier not present in hybrids strains. Investigating why this occurs might elucidate more about mechanisms involved in nuclear reprogramming.

Much remains to be learnt about how somatic nuclei are reprogrammed after being transferred into ooplasts. For example, what factors and signalling pathways are involved in altering the chromatin structure, methylation patterns, and gene expression during reprogramming? Is there a master trigger that induces a cascade of downstream events or does it take several factors working in parallel pathways to initiate reprogramming? This might be the case as the frequency of successful reprogramming is so low. How do subtle epigenetic differences from normal animals, such as methylation/acetylation patterns, contribute to the abnormalities that cloned animals often exhibit?

In summary, successful production of cloned animals by NT proved that somatic nuclei could reverse their developmental clock to recreate totipotency in the oocyte. The transferred nuclei must be reprogrammed in resetting of an embryonic transcriptional programme. Although NT remains the tool

of choice for studying reprogramming at a functional level, less technically demanding approaches may be helpful for dissecting reprogramming at the cellular, molecular and biological levels (Hochedlinger and Jaenisch, 2006).

Cell fusion: a reprogramming system with the challenge of tetraploidy

Cell fusion is the mechanism by which reprogramming occurs naturally; a haploid oocyte fuses with a haploid spermatozoan. Artificially induced cell fusion generates tetraploid cells which, due to their lack of contribution to chimeras and their perceived susceptibility to turn aneuploid and abnormal, are of limited therapeutic use (Tada *et al.*, 1997; Sullivan and Eggan, 2007). However, cell fusion is the only system yet to show reprogramming in humans (Cowan *et al.*, 2005), and if it was possible to harness cell enucleation strategies either by naturally occurring (erythrocyte enucleation or selective genome ejection systems seen in insects species such as fire-ants) or artificial means (cytoplast/whole cell fusions, or manual chromatin removal), this problem could be surmounted (Sullivan and Eggan, 2007).

Cell fusion, apart from being a potential therapy, has provided a model system where aspects of how cell-specific phenotypes are initiated and maintained can be examined in fusion products of different cell types (intertypic synkaryons). Monoclonal antibodies and polymorphisms between fusion partners can be used to study gene expression at the single cell level or in mass cultures at a biochemical and molecular level. Regulatory mechanisms governing cell fate and differentiation have been partially elucidated by studying differences among cell types in the frequency, kinetics, and patterns of gene expression. The results of both strategies applied to heterokaryons and cell hybrids show that the expression of genes in the nuclei of differentiated cells is remarkably plastic and susceptible to modulation by the cytoplasm (Boshart *et al.*, 1993). Isolation of genetically stable cell hybrids can be achieved using selection for transgenes integrated in, or against mutations occurring in, only one of the parental cell types. Generation of cell hybrids has elucidated three principles of cell differentiation (Boshart *et al.*, 1993): (i) trans-acting gene regulators are involved in cell differentiation; (ii) such regulators repress as well as activate cell-specific gene expression; and (iii) maintenance of the differentiated state is dependent on such factors.

In intertypic somatic hybrids, genes associated with specialized function are often shut down. Such repression is termed 'extinction'. Extinction is a commonly observed feature of intertypic hybridization (Davidson, 1974). One interesting example of hybridization provided the first direct evidence that telomere length determines proliferative capacity in human cells (Wright *et al.*, 1996). In immortal cell lines, the ends of the chromosomes (telomeres) are constitutively replenished by the ribonucleoprotein enzyme telomerase (Counter *et al.*, 1992), while in somatic cell types, telomere length is found to shorten with age (Lindsey *et al.*, 1991; Vaziri, 1997). Hybrids of immortal and somatic cells are found to have limited life span, and this is due to the extinction of the telomerase gene (Wright, 1996). Treating these cell hybrids with specific oligonucleotides results in telomere elongation. It is thought that telomere elongation reduces the probability of DNases cutting into essential regulatory and expressed sequences in chromosomal DNA and so extends the life span of the hybrids (Wright *et al.*, 1996).

Gene repression is far more commonly observed than activation (Baron *et al.*, 1996). However, it has been observed that activation of cell-type specific gene expression can also occur when different cell types are fused (Baron *et al.*, 1996). An interesting example of activation involves fusing erythroid cells at different developmental stages (Broyles, 1999). The phenotype of hybrid cells involves the retention of specific chromosomes (Weiss and Chaplain, 1971), and is dependent on the number of copies of the individual chromosomes retained. For example in hepatoma × fibroblast hybrids possessing only one copy of hepatic chromosomes, the hepatic phenotype is not observed; if, however, the hybrid contains two sets of hepatic chromosomes, the hepatic phenotype is present. Clearly a delicate equilibrium between positive and negative trans-acting factors mediates hybrid phenotype (Peterson and Wess, 1972). It is interesting to juxtapose these data with similar findings from imprinting experiments injecting transgenes containing differentially methylated regions (Reik *et al.*, 1999). Introduction of such genes alters the methylation status of the chromosomal DNA, also indicating a trans-acting mechanism with a delicate equilibrium (Reik *et al.*, 1999).

In summary, cell hybridization experiments have shown that trans-acting gene regulators control the differentiated state of a cell. Somatic cells may be reprogrammed by fusion with pluripotent stem cells; however, in this case, the persistence of ES cell-derived chromatin causes applicative and interpretive complications, i.e. the resulting tetraploid cells are of limited therapeutic use and it is still unknown whether the ES cell chromatin remaining in the fusion product is playing an active role in the perpetuation of the resultant phenotype.

iPS cell transduction: a technique to study reprogramming at the molecular level

There is currently much interest in the reprogramming community surrounding 'induced pluripotent stem (iPS) cell transduction' (Takahashi and Yamanaka, 2006) (**Figure 1**), a novel approach that uses four transcription factors to restore an ES cell-like phenotype to murine fibroblasts (Rodolfa and Eggan, 2006). By simply transducing murine fibroblast cultures with Moloney virus coding for four stem cell factors (Oct3/4, Sox2, Klf4 and c-Myc), it appears that a pluripotent stem cell-like state can be restored. This is particularly exciting when one considers that the techniques involved (cell culture and viral transduction) are commonly used in many laboratories worldwide already. New work on iPS cells has recently been published from three different laboratories (Rodolfa *et al.*, 2007). They showed iPS cells selected for Nanog expression can contribute to all tissue types including germ cells. Amazingly, the Nanog–iPS cells closely resemble ES cells in their epigenetic state as well as genetic activity (Okita *et al.*, 2007; Wernig *et al.*, 2007; Maherali *et al.*, 2007). Many laboratories worldwide can now use this method to elucidate

reprogramming mechanisms. Further published work with this technique is eagerly anticipated, as several questions have still to be answered: for example what cells are being transduced to generate these iPS cells? Can this be done with human cells? What is the molecular basis of reprogramming induced by the four factors? Is it the same process that happens during NT and cell fusion reprogramming? Can the implicated genes be activated and induce reprogramming without use of oncogenic virus (Surani, 2007)?

Screening for reprogramming factors

Reprogramming remains largely phenomenological, and efforts should now aim to dissect the mechanism at the molecular level (Hochedlinger and Jaenisch, 2006). Oocytes, preimplantation embryos, and pluripotent stem cells contain factors sufficient for reprogramming, and so constitute good material for identifying reprogramming factors (Hamatani *et al.*, 2004; Ko, 2006). Beyhan *et al.* (2007) reported global gene expression analysis of bovine NT, IVF embryos and donor somatic cells to characterize differences in their transcription profiles. They have found a small set of genes differentially expressed as well as genes of donor cells persistently expressed in NT embryos. Investigating gene expression changes that occur during or soon after reprogramming should elucidate the molecular mechanisms involved.

Another approach includes the use of mass spectrometry to identify reprogramming factors in cells and cell-derived extracts (Koziol *et al.*, 2007). Cell extracts have been shown to induce transient changes in gene expression and chromatin structure in differentiated cells (Dimitrov and Wolffe, 1996), which, if maintained, could possibly result in reprogramming. However, a caveat to these approaches is that the initial induction of reprogramming may only involve subtle changes in gene expression that then cumulatively elicit a pronounced effect. A more forceful approach would be to individually overexpress the four factors shown by Yamanaka and colleagues to reprogram differentiated cells (Takahashi and Yamanaka, 2006) and analyse the resulting genome-wide changes in gene expression. Alternatively, small molecule or RNAi screens could be performed to identify the important factors (Edwards, 2006).

Induction and maintenance of nuclear programmes has, for many years, been considered to be directed solely by proteins involved in gene regulation and morphogenic signalling. Many researchers have carried out reprogramming screens for proteins only to pull out generic chromatin remodeling factors. Additional candidates now need to be considered, including non-proteinaceous macromolecules. RNA, for example, has now emerged as a key player in a surprisingly large number of gene regulation studies. For example, the activity of X chromosomes in female mammals is controlled by non-coding RNAs such as *Xist* and *Tsix*. Furthermore, microRNAs (miRNAs), a large family of short non-coding RNAs (17–25 nucleotides) that mainly function to repress expression of their target genes, regulate blood development (Yekta *et al.* 2004). Tang *et al.* (2007) have recently showed a large proportion of the maternal genes are directly or indirectly under the control of miRNAs, which demonstrates that the maternal miRNAs are essential for the earliest stages of mouse embryonic development. It would not be surprising if non-coding RNA has further roles in specific and stable regulation of developmental programmes. miRNA may have an important role in nuclear reprogramming.

An alternative approach to studying artificial reprogramming, which could be expanded further, has been to study naturally induced reprogramming in lower vertebrates where it occurs successfully and more frequently and to look for common elements in more complex organisms. Unlike mammals, many fish and amphibia have the capacity to regenerate complex structures such as limbs after injury. Even mammals have this capacity in Msx1 expressing regions at the digit termini and more widely during early embryonic phases (Han *et al.*, 2003). This process involves cell migration and a change in cell phenotype in response to the injury. There are certain caveats here, however. It is hard to dissect process important for reprogramming from other processes such as the innate immune response, cell migration, and other consequences of injury. It is also unknown to what extent these processes are conserved in mammals. Still, dedifferentiation of cells to form proliferating progenitor cells is interesting, and systems such as skeletal muscle, limb and tail regeneration or dorsal iris epithelium during lens regeneration should be studied further with screens designed to find the key players involved.

The main challenge facing elucidation of nuclear reprogramming mechanisms using the conventional approaches, and potential solutions

The main problem with current studies investigating nuclear reprogramming mechanisms is the lack of material due to the low frequencies of reprogramming using artificial methods. Conventional approaches entail isolating and expanding reprogrammed cells in strongly selective culture conditions [e.g. in cell fusion experiments (Tada *et al.*, 1997; Cowan *et al.*, 2005) hybrid clones were isolated by antibiotic resistance and expanded]. Analysing such material, however, does not allow discrimination between the epigenetic changes necessary for the induction of reprogramming versus those that happen independently of such induction; i.e. it does not allow the study of reprogramming as it is happening.

How can the study of this process be facilitated? One strategy is to use easily reprogrammable cells, such as cells differentiated from ES cells in culture (Blelloch *et al.*, 2006; Silva *et al.*, 2006). Perhaps the initial focus should be on cultured cells instead of later primary cells, as these will still have strong epigenetic regulation, and thus would be harder to reprogram. Experiments with cultured cells should yield more reprogrammed material.

Additionally, it would be possible to use chromatin modifying drugs such as trichostatin A and 5-aza-2'-deoxycytidine to make the chromatin less condensed and more accessible. Factors required for activating the *Oct-3/4* gene are unknown, but recently it has been shown that two chromatin modifying drugs can activate the *Oct-3/4* gene in cells (Hattori *et al.*, 2004). These two drugs, trichostatin A (TSA) and 5-aza-2'-deoxycytidine

(5-aza-dC), which inhibit histone deacetylation and DNA methylation respectively, are thought to make the chromatin structure more open and consequently the *Oct-3/4* gene easier to activate. However, such drug treatment is quite toxic to the cells as well as being non-specific (these drugs reactivate many genes including those not associated with an ES cell phenotype (S Sullivan, unpublished data). Tsuji-Takayama *et al.* (2004) have recently shown that treatment of differentiated ES cells with a similar chemical to 5-aza-dC, called 5-azacytidine, causes the up-regulation of stem cell marker genes *Oct-3/4*, *Nanog* and *Sox2*. As with Hattori's work, the expression of genes associated with differentiated cells were not studied, and it is expected that these too will be up-regulated. It will be very interesting to screen for more specific drugs that increase the frequency of reprogramming.

Thirdly, although the reason is unknown, cell cycle synchronization by serum starvation makes murine embryonic fibroblasts (MEF) more easily reprogrammed both by NT (Campbell, 1996) or cell fusion (Sullivan *et al.*, 2006) This strategy could also facilitate reprogramming studies.

Can one learn about reprogramming and improve its efficiency by transposing conditions between the three reprogramming methods?

In order to learn from experiments using the three different methods to deduce the reprogramming mechanism(s) and improve their efficiencies, it is necessary to compare and contrast observations from them. At present, it is difficult to dissect the important events such as changes in gene regulation and chromatin structure during the reprogramming processes due to the inefficiency of all three methods, but some hints can be gathered from existing kinetic, gene expression, and cell cycle data. The kinetics of reprogramming appears to be very similar between NT and cell fusion. Somatic cell-derived transgenic Oct-3/4 is expressed within 24 h after NT and cell fusion (Sullivan and Egli, unpublished data). In contrast, reprogramming experiments using viral transduction have shown that stem cell genes *Alkaline Phosphatase*, *SSEA-1*, and *Nanog* are not highly expressed until 2–3 weeks post-infection (Blelloch *et al.*, 2007; Maherali *et al.* 2007; Meissner *et al.* 2007; Okita *et al.* 2007; Wernig *et al.* 2007), indicating that reprogramming proceeds at a slower pace with this method. The need to synthesize the four reprogramming genes *de novo* can only partially explain the slower kinetics of reprogramming using the viral transduction method. It is likely that other proteins that facilitate the induction of reprogramming during NT and cell fusion are missing, or that the entire transcriptional programme required for reprogramming, which is more completely expressed by the oocyte during NT or the ES cell during cell fusion, is vast and requires a substantial amount of time to execute. For example, demethylation of promoters of endogenous genes such as Oct-3/4 may occur very slowly during reprogramming by viral transduction if factors required for active demethylation are not produced as they are thought to be during NT (Yamazaki *et al.* 2006).

The two pluripotency genes used in the iPS cell viral transduction approach, *Oct-3/4* and *Sox2*, are expressed in oocytes (Avilion *et al.*, 2003; Monti *et al.*, 2006) and mouse ES cells (Yamanaka, 2007), suggesting that their roles in establishing and/or maintaining pluripotency are conserved in all three reprogramming approaches. Yamanaka posits that c-Myc may make the chromatin more accessible to transcription factors by binding to many sites in the genome and inducing histone deacetylation in addition to promoting self-renewal, as it does in murine ES cells (Cartwright *et al.* 2005; Yamanaka, 2007). c-Myc is expressed in oocytes (Naz *et al.* 1994) but is not highly expressed in mouse ES cells (Blelloch *et al.*, 2007). However, a functionally equivalent family member, n-Myc, is expressed and can substitute for c-Myc in iPS cell transduction (Blelloch *et al.*, 2007). Thus, Myc proteins may stimulate self-renewal in iPS cell transduction, cell fusion and NT. *Klf-4* is highly expressed in mouse ES cells (Yamanaka, 2007) and thus may play a role in reprogramming during cell fusion.

Cell cycle synchronization of the somatic cells into G_0/G_1 or G_2/M prior to NT or cell fusion increases the efficiency of reprogramming (Campbell *et al.*, 1996; Sullivan *et al.*, 2006). This effect is attributable to avoiding the aneuploidy or chromosomal damage risked by nuclear transfer or cell fusion during S phase. Yamanaka used unsynchronized cells in the iPS cell transduction experiments because active cell division is a requirement for infection by Moloney retrovirus. Egli and coworkers determined that a zygote arrested in mitosis can reprogram a somatic nucleus while an interphase zygote cannot (Egli *et al.*, 2007). A major difference between a mitotic zygote and an interphase zygote is that the nuclear membrane has broken down in the mitotic zygote. Therefore, it is possible that factors required for reprogramming are sequestered in the nucleus during interphase and released during mitosis. In cell fusion in mice, ES cells in G_2/M phase were the most effective at reprogramming, suggesting that key reprogramming activities at that stage of the cell cycle (Sullivan *et al.*, 2006).

Now there is the opportunity to use observations made in one method of reprogramming to try to improve the other methods. For example, will overexpressing some or all of the four Yamanaka factors in ES cells make reprogramming by cell fusion more efficient? The best evidence that this might be the case is given by Silva and coworkers. They reported elevated frequencies of reprogramming in a cell fusion system where *Nanog*, a pluripotency gene not necessary for iPS cell formation by viral transduction, was overexpressed in the ES cell fusion partner (Silva *et al.*, 2006). High Nanog levels may assist the induction of reprogramming indirectly as positive feedback circuits involving Nanog elevate Oct-3/4 and Sox2 levels (Loh *et al.*, 2006).

It will also be interesting to introduce *c-Myc* and *Klf-4* transgenically into cells to be reprogrammed by NT or cell fusion, to see if this increases the frequency of reprogramming; however, as these gene are both oncogenes, the resultant cells should be tested for epigenetic and genetic abnormalities. There is an additional caveat with this approach: what is learned from reprogramming genetically manipulated, cultured cells may not immediately inform the process of reprogramming normal primary somatic cells, which still have all epigenetic regulatory processes intact. It is, however, a first step towards reprogramming primary cells and should give enough material to untangle the various mechanisms.

Slow demethylation or chromatin re-structuring may be why Yamanaka's viral transduction method proceeds more slowly than NT or cell fusion. This seems likely, given that the other two methods have other factors that could potentially speed up these processes. For example, Yamazaki and coworkers found that even in NT, demethylation of the *Oct-4* promoter proceeds gradually and is probably a result of both active and passive mechanisms for demethylation (Yamazaki *et al.*, 2006). Yamanaka's four factors may not be sufficient to induce active demethylation, and may be dependent on the passive mechanism alone, causing slower reprogramming. Overexpression of de-novo methyl-transferase genes such as *Dnmt-1* or *Dnmt-3* might facilitate the process. Alternatively, if chromatin remodelling is the rate-limiting step, small molecule HDAC inhibitors could expedite reprogramming.

In the future, determining the list of genes that are up-regulated in ES cells during G_2/M phase or proteins that are localized in the nucleus during interphase in zygotes will significantly concentrate the search for genes necessary for reprogramming. Additionally, Yamanaka's work suggests that transcription factor libraries may be the most fruitful source of reprogramming factors.

Currently, it seems reasonable that all three reprogramming methods share a general mechanism involving chromatin remodelling to allow changes in gene expression as the first step, followed by changes to prevent cell death. The last step would be the induction of pluripotency. It also seems likely that the genes used to induce pluripotency are the same in all three methods, while there could be different molecular pathways to cell immortalization and altering DNA accessibility.

Conclusion

NT is the only reprogramming technique known not to require addition of foreign genes to induce restoration of developmental potential. Furthermore, it is still the only method can restore pluripotency without a high risk of oncogenesis. Thus, NT remains a very important system for studying reprogramming. Efficiency by this and the other two methods discussed is, however, still very low and the lack of material limits efforts to identify important factors for reprogramming induction. All three methods (NT, cell fusion, and iPS cell transduction) should be perused so that conditions optimal in one system can be implemented in the others to try to improve reprogramming frequencies. The four iPS cell factors can be introduced into cells that are to be used in NT and cell fusion experiments with the hope of increasing the frequency of reprogramming. It is hoped this will provide more material to study mechanisms and so help understanding of reprogramming. The scarcity of tissues and organs for transplantation, as well as the need for pluripotent stem cells to develop in-vitro models of human disease and development, compel further study of reprogramming mechanisms.

Acknowledgements

SS is funded by a fellowship from the Harvard Stem Cell Research Foundation. JI is funded by a fellowship from the New York Stem Cell Foundation. AU and HA are funded by Health and Labour Sciences Research Grants, Japan. The authors thank Esther Son, Kit Rodolfa, Katelyn Foley, and Gabriella Boulting for proofreading the manuscript.

References

Avilion AA, Nicolis SK, Pevny LH *et al.* 2003 Multipotent cell lineages in early mouse development depend on SOX2 function. *Genes and Development* **17**, 126–140.

Baron MD, Kamata Y, Barras V *et al.* 1996 The genome sequence of the virulent Kabete 'O' strain of rinderpest virus: comparison with the derived vaccine. *Journal of General Virology* **77**, 3041–3046.

Barton SC, Arney KL, Shi W *et al.* 2001 Genome-wide methylation patterns in normal and uniparental early mouse embryos. *Human Molecular Genetics* **10**, 2983–2987.

Beyhan Z, Ross PJ, Iager AE *et al.* 2007 Transcriptional reprogramming of somatic cell nuclei during preimplantation development of cloned bovine embryos. *Developmental Biology* **305**, 637–649.

Blelloch R, Venere M, Yen J, Ramalho-Santos M 2007 Generation of induced pluripotent stem cells in the absence of drug selection. *Cell Stem Cell* **1**, 245–247.

Blelloch R, Wang Z, Meissner A *et al.* 2006 Reprogramming efficiency following somatic cell nuclear transfer is influenced by the differentiation and methylation state of the donor nucleus. *Stem Cells* **24**, 2007–2013.

Boshart M, Nitsch D, Schutz G 1993 Extinction of gene expression in somatic cell hybrids – a reflection of important regulatory mechanisms? *Trends in Genetics* **9**, 240–245.

Brambrink T, Hochedlinger K, Bell G, Jaenisch R 2006 ES cells derived from cloned and fertilized blastocysts are transcriptionally and functionally indistinguishable. *Proceedings of the National Academy of Sciences of the USA* **103**, 933–938.

Briggs R, King TJ 1952 Transplantation of living nuclei from blastula cells into enucleated frogs' eggs. *Proceedings of the National Academy of Sciences of the USA* **38**, 455–463.

Broyles RH 1999 Use of somatic cell fusion to reprogram globin genes. *Seminars in Cell and Developmental Biology* **10**, 259–265.

Campbell KH 1999 Nuclear equivalence, nuclear transfer, and the cell cycle. *Cloning* **1**, 3–15.

Campbell KH, Loi P, Otaegui PJ, Wilmut I 1996 Cell cycle co-ordination in embryo cloning by nuclear transfer. *Reviews of Reproduction* **1**, 40–46.

Cartwright P, McLean C, Sheppard A *et al.* 2005 LIF/STAT3 controls ES cell self-renewal and pluripotency by a Myc dependent mechanism. *Development* **132**, 885–896.

Cibelli JB, Stice SL, Golueke PJ *et al.* 1998 Cloned transgenic calves produced from nonquiescent fetal fibroblasts. *Science* **280**, 1256–1258.

Counter CM, Avilion AA, LeFeuvre CE *et al.* 1992 Telomere shortening associated with chromosome instability is arrested in immortal cells which express telomerase activity. *EMBO Journal* **11**, 1921–1929.

Cowan CA, Atienza J, Melton DA, Eggan K 2005 Nuclear reprogramming of somatic cells after fusion with human embryonic stem cells. *Science* **309**, 1369–1373.

Davidson RL 1974 Gene expression in somatic cell hybrids. *Annual Review of Genetics* **8**, 195–218.

Di Giorgio FP, Carrasco MA, Siao MC *et al.* 2007 Non-cell autonomous effect of glia on motor neurons in an embryonic stem cell-based ALS model. *Nature Neuroscience* **10**, 608–614.

Dimitrov S, Wolffe AP 1996 Remodeling somatic nuclei in *Xenopus laevis* egg extracts: molecular mechanisms for the selective release of histones H1 and H1(0) from chromatin and the acquisition of transcriptional competence. *EMBO Journal* **15**, 5897–5906.

Edwards RG 2006 Genetics, epigenetics and gene silencing in differentiating mammalian embryos. *Reproductive BioMedicine Online* **13** 732–753.

Eggan K, Akutsu H, Loring J *et al.* 2001 Hybrid vigor, fetal overgrowth, and viability of mice derived by nuclear cloning and tetraploid embryo complementation. *Proceedings of the National*

Academy of Sciences of the USA **98**, 6209–6214.

Egli D, Rosains J, Birkhoff G, Eggan K. 2007 Developmental reprogramming after chromosome transfer into mitotic mouse zygotes. *Nature* **447**, 679–685.

Evans MJ, Kaufman MH 1981 Establishment in culture of pluripotential cells from mouse embryos. *Nature* **292**, 154–156.

Fulka J Jr, First NL, Moor RM 1996 Nuclear transplantation in mammals: remodelling of transplanted nuclei under the influence of maturation promoting factor. *Bioessays* **18**, 835–840.

Gridelli B, Remuzzi G 2000 Strategies for making more organs available for transplantation. *New England Journal of Medicine* **343**, 404–410.

Gurdon JB 1968 Nucleic acid synthesis in embryos and its bearing on cell differentiation. *Journal of Embryology and Experimental Morphology* **20**, 401–414.

Gurdon JB, ElsdaleTR, Fischberg M. 1958 Sexually mature individuals of *Xenopus laevis* from the transplantation of single somatic nuclei. *Nature* **182**, 64–65.

Hakelien AM, Landsverk HB, Robl JM *et al.* 2002 Reprogramming fibroblasts to express T-cell functions using cell extracts. *Nature Biotechnology* **20**, 460–466.

Hamatani T, Carter GM, Sharov AA *et al.* 2004 Dynamics of global gene expression changes during mouse preimplantation development. *Developmental Cell* **6**, 117–131.

Han M, Yang X, Farrington JE, Muneoka K 2003 Digit regeneration is regulated by Msx1 and BMP4 in fetal mice. *Development* **130**, 5123–5132.

Hattori N, Nishino K, Ko Y *et al.* 2004 Epigenetic control of mouse Oct-3/4 gene expression in embryonic stem cells and trophoblast stem cells. *Journal of Biological Chemistry* **279**, 17063–17069.

Hochedlinger K, Jaenisch R 2006 Nuclear reprogramming and pluripotency. *Nature* **441**, 1061–1067.

Hochedlinger K, Jaenisch R 2002 Nuclear transplantation: lessons from frogs and mice. *Current Opinion in Cell Biology* **14**, 741–748.

Kass SU, Wolffe AP 1998 DNA methylation, nucleosomes and the inheritance of chromatin structure and function. *Novartis Foundation Symposium* **214**, 36–50.

Kato K, Gurdon JB 1993 Single-cell transplantation determines the time when *Xenopus* muscle precursor cells acquire a capacity for autonomous differentiation. *Proceedings of the National Academy of Sciences of the USA* **90**, 1310–1314.

Kato Y, Tani T, Sotomaru Y *et al.* 1998 Eight calves cloned from somatic cells of a single adult. *Science* **282**, 2095–2098.

Kelly SJ 1977 Studies of the developmental potential of 4- and 8-cell stage mouse blastomeres. *Journal of Experimental Zoology* **200**, 365–376.

Kikyo N, Wade PA, Guschin D *et al.* 2000 Active remodeling of somatic nuclei in egg cytoplasm by the nucleosomal ATPase ISWI. *Science* **289**, 2360–2362.

Ko SHM 2006 Expression profiling of the mouse early embryo: reflections and perspectives. *Developmental Dynamics* **235**, 2437–2448.

Koziol MJ, Garrett N, Gurdon JB 2007 Tpt1 activates transcription of Oct3/4 and nanog in transplanted somatic nuclei. *Current Biology* **17**, 801–807.

Lindsey J, McGill NI, Lindsey LA, Green *et al.* 1991 In-vivo loss of telomeric repeats with age in humans. *Mutation Research* **256**, 45–48.

Loh YH, Wu Q, Chew JL *et al.* 2006 The Oct4 and Nanog transcription network regulates pluripotency in mouse embryonic stem cells. *Nature Genetics* **38**, 431–440.

Maherali N, Sridharan R, Xie W *et al.* 2007 Global epigenetic remodeling in directly reprogrammed fibroblasts. *Cell Stem Cell* **1**, 55–70.

Martinez-Balbas MA, Dey A, Rabindran SK *et al.* 1995 Displacement of sequence-specific transcription factors from mitotic chromatin. *Cell* **83**, 29–38.

Matsui YK, Zsebo K, Hogan BL 1992 Derivation of pluripotential embryonic stem cells from murine primordial germ cells in culture. *Cell* **70**, 841–847.

McGrath J, Solter D 1984 Inability of mouse blastomere nuclei transferred to enucleated zygotes to support development in vitro. *Science* **226**, 1317–1319.

Meissner A, Jaenisch R 2006 Mammalian nuclear transfer. *Developmental Dynamics* **235**, 2460–2469.

Meissner A, Wernig M, Jaenisch R 2007 Direct reprogramming of genetically unmodified fibroblasts into pluripotent stem cells. *Nature Biotechnology* **25**, 1177–1181.

Monk M, Boubelik M, Lehnert S 1987 Temporal and regional changes in DNA methylation in the embryonic, extraembryonic and germ cell lineages during mouse embryo development. *Development* **99**, 371–382.

Monti M, Garagna S, Redi C, Zuccotti M 2006 Gonadotropins affect Oct-4 gene expression during mouse oocyte growth. *Molecular Reproduction and Development* **73**, 685–691.

Naz RK, Kumar G, Minhas BS 1994 Expression and role of c-myc protooncogene in murine preimplantation embryonic development. *Journal of Assisted Reproduction and Genetics* **11**, 208–216.

Ogura A, Inoue K, Ogonuki N *et al.* 2000 Production male cloned mice fresh, cultured, and cryopreserved immature Sertoli cells. *Biology of Reproduction* **62**, 1579–1584.

Okita K, Ichisaka T, Yamanaka S 2007 Generation of germline-competent induced pluripotent stem cells. *Nature* **448**, 313–317.

Perreault SD 1992 Chromatin remodeling in mammalian zygotes. *Mutation Research* **296**, 43–55.

Peterson JA, Wess MC 1972 Expression of differentiated functions in hepatoma cell hybrids: induction of mouse albumin production in rat hepatoma-mouse fibroblast hybrids. *Proceedings of the National Academy of Sciences of the USA* **69**, 571–575.

Reik W, Kelsey G, Walter J 1999 Dissecting de novo methylation. *Nature Genetics* **23**, 380–382.

Resnick JL, Bixler LS, Cheng L, Donovan PJ 1992 Long-term proliferation of mouse primordial germ cells in culture. *Nature* **359**, 550-551.

Ribbert H 1911 *Das Karzinom des Menschen/Human Cancer*. Friedrich Cohen, Bonn.

Rideout WM 3rd, Eggan K, Jaenisch R 2001 Nuclear cloning and epigenetic reprogramming of the genome. *Science* **293**, 1093–1098.

Rodolfa KT, Eggan K 2006 A transcriptional logic for nuclear reprogramming. *Cell* **126**, 652–655.

Rodolfa K, Di Giorgio FP, Sullivan S 2007 Defined reprogramming: a vehicle for changing the differentiated state. *Differentiation* **75**, 577–579.

Schultz RM, Davis W Jr, Stein P *et al.* 1999 Reprogramming of gene expression during preimplantation development. *Journal of Experimental Zoology* **285**, 276–282.

Silva J, Chambers I, Pollard S, Smith A 2006 Nanog promotes transfer of pluripotency after cell fusion. *Nature* **441**, 997–1001.

Stojkovic M, Stojkovic P, Leary C *et al.* 2005 Derivation of a human blastocyst after heterologous nuclear transfer to donated oocytes. *Reproductive BioMedicine Online* **11**, 226–231.

Sullivan S, Eggan K 2007 The potential of cell fusion for human therapy. *Stem Cell Reviews* **2**, 341–350.

Sullivan S, Pells S, Hooper M *et al.* 2006 Nuclear reprogramming of somatic cells by embryonic stem cells is affected by cell cycle stage. *Cloning Stem Cells* **8**, 174–188.

Surani MA 2007 Afterword. In: Sullivan S, Chad CA, Eggan K (eds) *Human Embryonic Stem Cells: The Practical Handbook*. John Wiley and Sons, Ltd, Chichester, UK, 389–391.

Surani MA 1999 Reprogramming a somatic nucleus by trans-modification activity in germ cells. *Seminars in Cell and Developmental Biology* **10**, 273–277.

Tada M, Takahama Y, Abe K *et al.* 2001 Nuclear reprogramming of somatic cells by in vitro hybridization with ES cells. *Current Biology* **11**, 1553–1558.

Tada M, Tada T, Lefebvre L *et al.* 1997 Embryonic germ cells induce epigenetic reprogramming of somatic nucleus in hybrid cells. *EMBO Journal* **16**, 6510–6520.

Takahashi K, Yamanaka S 2006 Induction of pluripotent stem cells from mouse embryonic and adult fibroblast cultures by defined

factors. *Cell* **126**, 663–676.
Tang F, Kaneda M, OCarroll D *et al.* 2007 Maternal microRNAs are essential for mouse zygotic development. *Genes and Development* **21**, 644–648.
Tsuji-Takayama K, Inoue T, Ijiri Y *et al.* 2004 Demethylating agent, 5-azacytidine, reverses differentiation of embryonic stem cells. *Biochemical and Biophysical Research Communications* **323**, 86–90.
Vaziri H, West MD, Allsopp RC *et al.* 1997 ATM-dependent telomere loss in aging human diploid fibroblasts and DNA damage lead to the post-translational activation of p53 protein involving poly(ADP-ribose) polymerase. *EMBO Journal* **16**, 18–33.
Verlinsky Y, Strelchenko N, Kukharenko V *et al.* 2005 Human embryonic stem cell lines with genetic disorders. *Reproductive BioMedicine Online* **10**, 105–110.
Wakayama T, Tabar V, Rodriguez I *et al.* 2001 Differentiation of embryonic stem cell lines generated from adult somatic cells by nuclear transfer. *Science* **292**, 740–743.
Wakayama T, Tateno H, Mombaerts P, Yanagimachi R 2000 Nuclear transfer into mouse zygotes. *Nature Genetics* **24**, 108–109.
Wakayama T, Perry AC, Zuccotti M *et al.* 1998 Full-term development of mice from enucleated oocytes injected with cumulus cell nuclei. *Nature* **394**, 369–374.
Weismann A 1893 The Germ-Plasm: A Theory of Heredity. Charles Scribner's Sons, New York.
Weiss MC, Chaplain M 1971 Expression of differentiated functions in hepatoma cell hybrids: reappearance of tyrosine aminotransferase inducibility after the loss of chromosomes. *Proceedings of the National Academy of Sciences of the USA* **68**, 3026–3030.
Wernig M, Meissner A, Foreman R *et al.* 2007 In vitro reprogramming of fibroblasts into a pluripotent ES-cell-like state. *Nature* **448**, 318–324.
Willadsen SM 1986 Nuclear transplantation in sheep embryos. *Nature* **320**, 63–65.
Wilmut I, Schnieke AE, McWhir J *et al.* 1997 Viable offspring derived from fetal and adult mammalian cells. *Nature* **385**, 810–813.
Wobus AM, Boheler KR 2005 Embryonic stem cells: prospects for developmental biology and cell therapy. *Physiological Reviews* **85**, 635–678.
Wright WE, Brasiskyte D, Piatyszek MA, Shay JW 1996 Experimental elongation of telomeres extends the lifespan of immortal × normal cell hybrids. *EMBO Journal* **15**, 1734–1741.
Yamanaka S 2007 Strategies and new developments in the generation of patient-specific pluripotent stem cells. *Cell Stem Cell* **1**, 39–44.
Yamazaki Y, Fujita TC, Low EW *et al.* 2006 Gradual DNA demethylation of the Oct4 promoter in cloned mouse embryos. *Molecular Reproduction and Development* **73**, 180–188.
Yekta S, Shih IH, Bartel DP 2004 MicroRNA-directed cleavage of HOXB8 mRNA. *Science* **304**, 594–596.

Received 27 July 2007; refereed 12 September 2007; accepted 17 October 2007.

The fusing ability of sperm is bestowed by CD9-containing vesicles released from eggs in mice

Kenji Miyado*[††§], Keiichi Yoshida[‡¶], Kazuo Yamagata[∥], Keiichi Sakakibara*, Masaru Okabe**, Xiaobiao Wang*, Kiyoko Miyamoto*, Hidenori Akutsu*, Takahiko Kondo*, Yuji Takahashi*, Tadanobu Ban[††], Chizuru Ito[¶], Kiyotaka Toshimori[¶], Akihiro Nakamura*, Masahiko Ito*, Mami Miyado*, Eisuke Mekada**, and Akihiro Umezawa*

*National Center for Child Health and Development, 2-10-1 Okura, Setagaya, Tokyo 157-8535, Japan; [†]School of Biomedical Science, Tokyo Medical and Dental University, Yushima, Bunkyo, Tokyo 113-8510, Japan; [¶]Graduate School of Medicine, Chiba University, 1-8-1 Inohana, Chuo-ku, Chiba 260-8670, Japan; [∥]Center for Developmental Biology, RIKEN Kobe Institute, 2-2-3 Minatojima-minamimachi, Chuo-ku, Kobe, Hyogo 650-0047, Japan; and **Research Institute for Microbial Diseases, and [††]Faculty of Medicine, Osaka University, 3-1 Yamadaoka, Suita, Osaka 565-0871, Japan

Edited by Ryuzo Yanagimachi, University of Hawaii, Honolulu, HI, and approved July 8, 2008 (received for review November 8, 2007)

Membrane fusion is an essential step in the encounter of two nuclei from sex cells—sperm and egg—in fertilization. However, aside from the involvement of two molecules, CD9 and Izumo, the mechanism of fusion remains unclear. Here, we show that sperm–egg fusion is mediated by vesicles containing CD9 that are released from the egg and interact with sperm. We demonstrate that the $CD9^{-/-}$ eggs, which have a defective sperm-fusing ability, have impaired release of CD9-containing vesicles. We investigate the fusion-facilitating activity of CD9-containing vesicles by examining the fusion of sperm to $CD9^{-/-}$ eggs with the aid of exogenous CD9-containing vesicles. Moreover, we show, by examining the fusion of sperm to $CD9^{-/-}$ eggs, that hamster eggs have a similar fusing ability as mouse eggs. The CD9-containing vesicle release from unfertilized eggs provides insight into the mechanism required for fusion with sperm.

fertilization | membrane fusion | EGFP | exosome

Fertilization is an essential process that naturally produces a cell capable of developing into a new individual. It consists of sequential events, including membrane fusion of sperm and egg (1). Despite the importance of understanding fertilization in controlling human reproduction and preserving endangered species, the molecular basis underlying the fusion remains a mystery, however. Previously, we reported that a tetraspan-membrane protein (tetraspanin), CD9, is expressed on the egg plasma membrane and is required for sperm–egg fusion (2–4). A role of CD9 in other fusion events also has been demonstrated (5). When sperm are added to eggs from $CD9^{-/-}$ females, the sperm bind to the egg plasma membrane normally, but fusion is severely impaired (2–4). Two recent observations suggest that CD9 plays a role in the organization of egg membrane. First, CD9 is transferred from the egg to the fertilizing sperm present in the perivitelline space (PVS) (6), suggesting the involvement of a process similar to trogocytosis, a mechanism of cell-to-cell contact-dependent transfer of membrane fragments (7). Second, CD9 deficiency alters the length and density of microvilli on the egg plasma membrane (8). CD9 is also known to be a component of exosomes, membrane vesicles released from a wide range of cells (9, 10). Despite its relationship to CD9, the involvement of exosome release in sperm–egg fusion remains unknown. In the present study, we analyzed the potential of enhanced green fluorescent protein (EGFP)-tagged CD9 (CD9-EGFP) as a reporter protein to study sperm–egg fusion in living mouse eggs.

Results

To observe the movement of CD9 during sperm–egg fusion, we generated a transgenic mouse line that expressed CD9-EGFP only in eggs (Fig. 1*A*), and converted to the genetic background of $CD9^{-/-}$ mice by mating mice. Western blot analysis using anti-CD9 monoclonal antibody (mAb) revealed that an expected CD9-EGFP with a molecular mass of 51 kDa (CD9 and EGFP

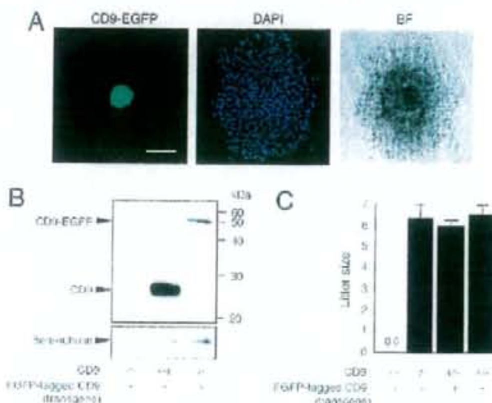

Fig. 1. Generation of mice expressing CD9-EGFP in eggs. (*A*) CD9-EGFP specifically expressed in eggs with mouse ZP3-promoter. Cumulus oocyte complex from $Tg^{+}CD9^{+/+}$ oviducts was collected at 14 h after injection of human chorionic gonadotropin. Nuclei of an egg and cumulus cells were counterstained with DAPI. (*Left*) CD9-EGFP. (*Center*) DAPI. (*Right*) Bright field. Scale bar: 100 μm. (*B*) Western blot analysis for eggs collected from $CD9^{-/-}$, $CD9^{+/+}$, and $Tg^{+}CD9^{-/-}$ mice. The same amounts, including 30 eggs of each lysate, were examined by anti-CD9 and anti-beta-tubulin mAbs (internal control). (*C*) Litter sizes of $CD9^{-/-}$ ($n = 31$), $Tg^{+}CD9^{-/-}$ ($n = 35$), $Tg^{+}CD9^{+/-}$ ($n = 16$), and $CD9^{+/-}$ mice ($n = 15$) (mean ± SEM). The numbers of females examined are in parentheses.

contributing to 24 and 27 kDa, respectively) was expressed in the eggs collected from $Tg^{+}CD9^{-/-}$ mice; however, the amount of CD9-EGFP expressed in $CD9^{-/-}$ eggs was estimated to be 10% of that of endogenous CD9 in the $CD9^{+/+}$ eggs (Fig. 1*B*). Despite the small amount of CD9-EGFP expressed in eggs, CD9-EGFP demonstrated the ability to reverse the sterility of $CD9^{-/-}$ females (Fig. 1*C*). The numbers of pups obtained from $Tg^{+}CD9^{-/-}$ females (6.4 ± 0.5) were similar to those from

Author contributions: K. Miyado, K. Yamagata, M.O., and A.U. designed research; K. Miyado, K. Yoshida, K.S., X.W., K. Miyamoto, H.A., T.K., Y.T., T.B., C.I., A.N., M.I., and M.M. performed research; K. Miyado contributed new reagents/analytic tools; K. Miyado, K. Yoshida, H.A., K.T., E.M., and A.U. analyzed data; and K. Miyado wrote the paper.

The authors declare no conflicts of interest.

This article is a PNAS Direct Submission.

Freely available online through the PNAS open access option.

[‡]K. Miyado and K. Yoshida contributed equally to this work.

[§]To whom correspondence should be addressed. E-mail: kmiyado@nch.go.jp.

This article contains supporting information online at

© 2008 by The National Academy of Sciences of the USA

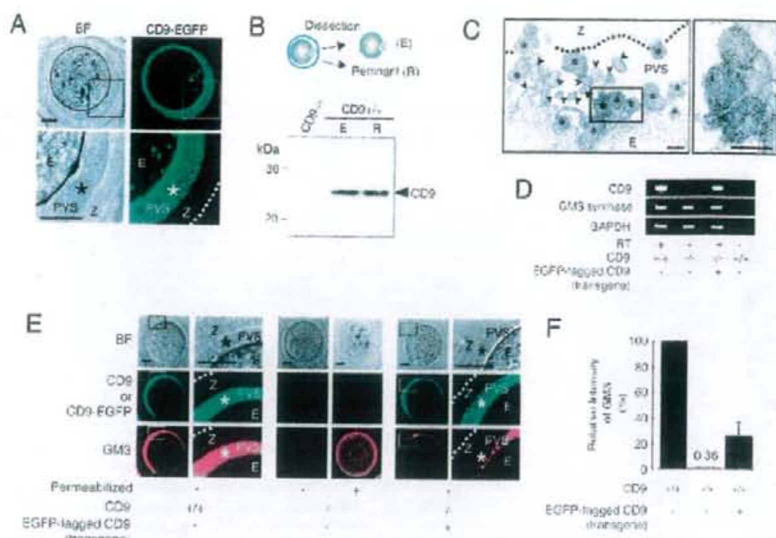

Fig. 2. Identification of secretory vesicles containing CD9 from unfertilized eggs. *A*, A single confocal image showing CD9-EGFP in unfertilized Tg^{+}CD9$^{-/-}$ eggs (E), including the PVS (*), zona pellucida (Z), and the outer margin of the zona pellucida (dotted line). (*Left*) Bright field. (*Right*) CD9-EGFP. *Lower* are enlarged images of the boxed areas. (*B*) Western blot analysis for eggs mechanically fractionated as shown in the diagram: zona-intact CD9$^{-/-}$ eggs (E) (10 eggs per lane) and zona-free CD9$^{+/+}$ eggs (10 eggs per lane). The medium (R) containing the remnant material from 40 eggs treated with a piezo manipulator was loaded in each lane. (*C*) Immunoelectron-microscopic analysis of CD9$^{+/+}$ eggs. The zona-intact CD9$^{+/+}$ eggs were examined using anti-CD9-mAb and 5-nm gold beads conjugated with anti-rat IgG Ab. Left panel: Image including CD9-containing vesicles (*), microvilli (arrowheads), zona pellucida (Z), perivitelline space (PVS), and egg (E). (*Right*) An enlarged image of the boxed region in the left panel. Scale bar: 200 nm. (*D*) RT-PCR for CD9, GM3 synthase, and glyceraldehyde-3-phosphate dehydrogenase transcripts in CD9$^{+/+}$, CD9$^{-/-}$, and Tg^{+}CD9$^{-/-}$ eggs. The same amounts, including 50 eggs in each reaction, were examined. The right end lanes are negative controls in which RT was removed from reactions of wild-type eggs. (*E*) Localization of GM3 and CD9 in CD9$^{+/+}$, CD9$^{-/-}$, and Tg^{+}CD9$^{-/-}$ eggs. (*Left*) Wild-type. (*Middle*) CD9$^{-/-}$. (*Right*) Tg^{+}CD9$^{-/-}$. Right-side of the sets of wild-type and Tg^{+}CD9$^{-/-}$ eggs are enlarged images of the boxed regions. The live eggs were examined, and the internal localization of GM3 in CD9$^{-/-}$ eggs was examined under fixed, permeabilized conditions. (*F*) Comparison of the fluorescent intensities of GM3 stained by antibody in wild-type (n = 10), CD9$^{-/-}$ (n = 9), and Tg^{+}CD9$^{-/-}$ eggs (n = 10) (mean ± SEM). The average values of the wild-type eggs were set to 100%.

Tg^{+}CD9$^{+/-}$ and CD9$^{+/-}$ females (6.0 ± 0.2 and 6.5 ± 0.5) and greater than those from CD9$^{-/-}$ females (0.0 ± 0.0). The CD9$^{+/-}$ females did not exhibit any loss in fertility that could cause a reduction of litter size relative to that of the CD9$^{+/+}$ females (4). Furthermore, the transgene had no effect on normal fertility. These results demonstrate that transgenically expressed CD9-EGFP can compensate for the loss of intrinsic CD9 and yield eggs with the ability to fuse with sperm.

Based on the foregoing evidence, we observed the subcellular localization of CD9-EGFP in "living" Tg^{+}CD9$^{-/-}$ eggs (Fig. 2*A*). As expected, confocal microscopic analysis allowed the visualization of two types of CD9-EGFP localization: intense on the plasma membrane and also in the cytoplasm. Unexpectedly, we found loosely filled, noncompacted CD9-EGFP in the PVS, a space formed between the zona pellucida and the plasma membrane of the egg. The localization of CD9 outside the eggs also was confirmed by Western blot analysis using anti-CD9 mAb (Fig. 2*B*). As shown in the diagram, CD9$^{+/+}$ eggs were mechanically fractionated into denuded eggs and other components (R) using a piezo manipulator (11). The fraction R, containing the zona pellucida and the components in the PVS, was centrifuged and subjected to Western blot analysis. The amount of CD9 in the remnant material from 40 eggs was found to be densitometrically equal to that of 10 zona-free eggs, demonstrating an estimated relative abundance of CD9 in the remnant of 20% per egg. Subsequently, we performed immunoelectron-microscopic analysis on the CD9$^{+/+}$ eggs. We identified the vesicles bound to gold particles inside the PVS (Fig. 2*C*). The sectioned microvilli contained a branched network of actin filaments, whereas the variously sized vesicles (50–250 nm in diameter) had uniformly dense materials rather than actin filaments. We also compared CD9$^{+/+}$, Tg^{+}CD9$^{-/-}$, and CD9$^{-/-}$ eggs by electron-microscopic analysis [supporting information (SI) Fig. S1]. The accumulation of vesicles in the PVS in the Tg^{+}CD9$^{-/-}$ eggs was comparable to that in the CD9$^{+/+}$ eggs, whereas it was not seen in the CD9$^{-/-}$ or germinal vesicle-staged CD9$^{+/+}$ eggs. These results indicate that 20% of the total amount of CD9 is stored as vesicles in the PVS during meiosis.

We next examined the expression of ganglioside GM3, identified as a CD9-associated molecule (12) and a component of exosomes (10), in CD9$^{+/+}$, CD9$^{-/-}$, and Tg^{+}CD9$^{-/-}$ eggs. First, we confirmed the expression of GM3 synthase (ST3GalV/SAT-1) (13) in these eggs by RT-PCR (Fig. 2*D*). Then we investigated the localization of GM3 by immunostaining these live eggs with anti-GM3 mAb (Fig. 2*E*). This antibody has been demonstrated to recognize GM3 in the plasma membrane of cells without treatment for permeabilization (14). Finally, we measured the fluorescent intensities of GM3 in these live eggs (Fig. 2*F*). As expected, in wild-type eggs, GM3 was colocalized with CD9 in the PVS and plasma membrane (Fig. 2*E Left* and Fig. 2*F*). In contrast, in CD9$^{-/-}$ eggs, the fluorescent intensities of GM3 were decreased dramatically in the PVS and plasma membrane (0.4% ± 0.2%, relative to 100% for the CD9$^{+/+}$ eggs), consistent with the loss of CD9 (Fig. 2*E Center* and Fig. 2*F*), whereas GM3 could be detected in the cytoplasm of CD9$^{-/-}$ eggs that had been permeabilized by a detergent after fixation. Moreover, the expression of CD9-EGFP reversed the decrease of GM3 in the PVS and plasma membrane of CD9$^{-/-}$ eggs (25.6 ± 10.7%) (Fig. 2*E Right* and Fig. 2*F*), corresponding to the amount of CD9-EGFP quantified by Western blot analysis (Fig. 1*B*). In addition, electron-microscopic analysis revealed that the number of characteristic membrane structures, termed microvilli (1), were significantly decreased in the CD9$^{-/-}$ eggs compared with the CD9$^{+/-}$ eggs (Fig. S2 *A* and *B*). The numbers of microvilli were increased by ≈50% by the expression of CD9-EGFP in the CD9$^{-/-}$ eggs. The analyses of three types of eggs indicate that CD9- and GM3-containing vesicle release is linked to microvilli formation.

We next investigated the involvement of CD9-containing vesicles in sperm–egg fusion (Fig. 3). We found that, based on the length of microvilli (Fig. S2*C*), zona-intact Tg^{+}CD9$^{-/-}$ eggs can be categorized into two groups (Fig. 3*A*). From single

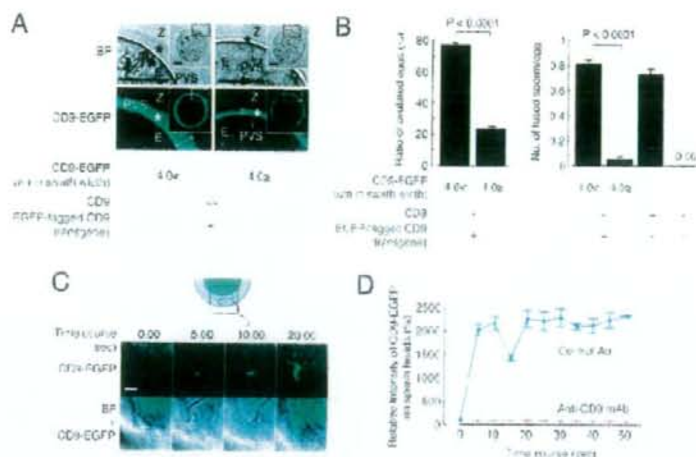

Fig. 3. Involvement of CD9-containing vesicles in sperm–egg fusion. (*A*) Categorization of Tg^{+}CD9$^{-/-}$ eggs (E) into two groups according to the thickness of CD9-EGFP in the PVS (*) and the inner region of the zona pellucida (Z) (>4.0 μm or ≤ 4.0 μm), indicated by double-headed lines. The boxed regions in *Insets* are enlarged. Scale bar: 20 μm. (*B*) Comparison of the fusing ability of two groups of Tg^{+}CD9$^{-/-}$ eggs with wild-type sperm. Left graph: Ratio of two groups of Tg^{+}CD9$^{-/-}$ eggs ovulated from 12 females (mean ± SEM). Right graph: Number of sperm fused per egg in two groups of zona-intact Tg^{+}CD9$^{-/-}$ eggs ovulated from 12 females (>4.0 μm, n = 204; ≤4.0 μm, n = 66) (mean ± SEM). CD9$^{+/+}$ (n = 120) and CD9$^{-/-}$ (n = 112) served as positive and negative controls, respectively. (*C* and *D*) Monitoring of the association of egg CD9-containing vesicles with wild-type sperm. Tg^{+}CD9$^{-/-}$ eggs were incubated with the sperm and monitored immediately after the sperm penetrated the zona pellucida under the presence of anti-CD9 mAb (boxed region). The values were calculated from data scanning by confocal microscopy (15 sperm in triplicate dishes) Blue: Preimmune rat IgG. Red: Anti-CD9 mAb (KMC8) (mean ± SEM). The average values of the fluorescent intensities of CD9-EGFP at 0 s were set to 100%, and the final concentration of antibodies was adjusted to 50 μg/ml. Scale bar, 5 μm.

confocal images sectioned through the largest diameter, the accumulation of CD9-EGFP from the plasma membrane to the inner region of the zona pellucida was >4.0 μm in swath width in one group and ≤ 4.0 μm in the other group. The accumulation of CD9-EGFP was predicted to show that CD9-containing vesicles are more highly accumulated within the PVS in the >4.0-μm group compared with the ≤ 4.0-μm group. Comparing the ratio of these two groups in Tg^{+}CD9$^{-/-}$-ovulated eggs revealed a much higher percentage of the >4.0-μm group (77.0 ± 1.3% vs.23.7 ± 1.5%) (Fig. 3*B Left*). Therefore, we focused on the heterogeneity of CD9-EGFP accumulation within the PVS and determined the ratio of the two groups in zona-intact Tg^{+}CD9$^{-/-}$ eggs that successfully fused with the sperm 6 h after insemination. The >4.0-μm group of Tg^{+}CD9$^{-/-}$ eggs showed higher activity for fusion with sperm (0.81 ± 0.04 sperm fused per egg), compared with the ≤40-μm group of Tg^{+}CD9$^{-/-}$ eggs (0.05 ± 0.03) and the CD9$^{-/-}$ eggs (0.00 ± 0.00), and comparable activity to that of wild-type eggs (0.73 ± 0.04) (Fig. 3*B Right*). The average activity of all Tg^{+}CD9$^{-/-}$ eggs (0.72 ± 0.03 sperm fused per egg) was equal to that of wild-type eggs (0.73 ± 0.04 sperm fused per egg). The difference between the two groups of Tg^{+}CD9$^{-/-}$ eggs was statistically significant (Fig. 3*B*). These results suggest that the quantities of CD9-containing vesicles, as assessed by the swath width of CD9-EGFP, are strongly correlated with the frequency of sperm–egg fusion.

To detect the association between sperm and CD9-containing vesicles, we serially monitored the wild-type sperm that penetrated the zona pellucida of the Tg^{+}CD9$^{-/-}$ eggs (Fig. 3 *C* and *D*). As shown in the diagram, we began monitoring the sperm immediately after the head portion of sperm penetrated the zona pellucida of the Tg^{+}CD9$^{-/-}$ eggs (Fig. 3*C Upper*, boxed area in the diagram). Soon after we began to monitor the sperm, the fluorescent intensities of CD9-EGFP on the sperm heads increased and then decreased rapidly between 0 s and 15 s, then increased again, reaching a maximum at 20 s. At this point, the CD9-EGFP fully covered the surface of the sperm heads. In contrast, when the sperm were incubated with Tg^{+}CD9$^{-/-}$ eggs in the medium containing anti-CD9 mAb, no increase in intensity of CD9-EGFP on the sperm heads was detected. Anti-CD9 mAbs have been reported to inhibit sperm–egg fusion (4, 15, 16). Our findings demonstrate that the anti-CD9 mAb inhibited the association of sperm with CD9-containing vesicles in parallel to inhibition of sperm–egg fusion.

To determine whether CD9-containing vesicles are capable of initiating sperm–egg fusion, we incubated the sperm with CD9$^{-/-}$ eggs in medium containing the vesicles collected from CD9$^{+/+}$ eggs (Fig. 4 and Fig. S3). To restrict the source of CD9 into the vesicles from the CD9$^{+/+}$ eggs, we used sperm collected from the epididymis of CD9$^{-/-}$ males. We estimated the capability of the vesicles to influence fusion by counting the number of sperm fused with CD9$^{-/-}$ eggs. As shown in the experimental design, after the zona pellucida was removed from the CD9$^{-/-}$ eggs, the eggs were incubated with sperm in the medium containing the vesicles (Fig. 4*A*). When examined at 1 h after incubation, the sperm were seen to be capable of fusing with CD9$^{-/-}$ eggs after co-incubation with the vesicles (Fig. 4*A Center*), indicating restoration of the fusibility of CD9$^{-/-}$ eggs with the sperm (0.58 ± 0.07 sperm fused per egg) (Fig. 4*B*). We detected further evidence of sperm–egg fusion in the CD9$^{-/-}$ eggs from which a second polar body had been extruded. In contrast, we did not detect improved fusibility of sperm with eggs in medium depleted of CD9-containing vesicles using beads conjugated with anti-CD9 mAb (Fig. 4*A Right* and *B*). After treatment with the beads, the quantity of CD9 in the depleted medium was significantly decreased, to 16% of the untreated medium (Fig. 4*C*). In addition, CD9$^{-/-}$ remnants failed to rescue the fusing ability of CD9$^{-/-}$ eggs. These findings indicate that the association with CD9-containing vesicles renders the sperm capable of fusing with eggs without endogenous CD9 expression. We estimated the relative abundance of CD9 in the remnant as 18% of the total amount in the eggs (Fig. 4*C*). We further found

PNAS PNAS PNAS

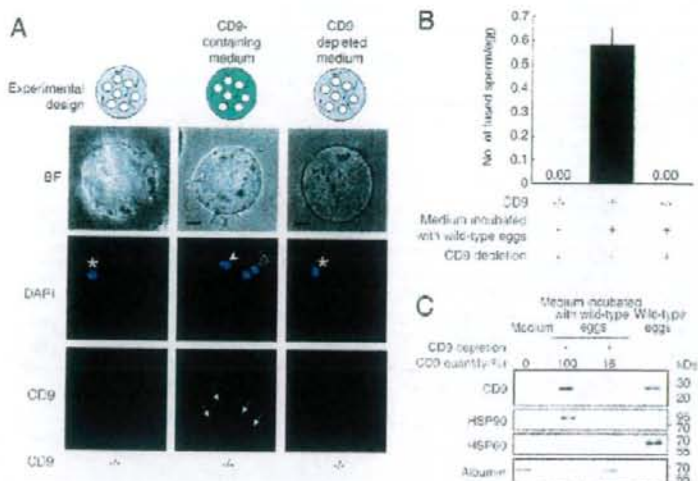

Fig. 4. Identification of fusion-facilitating activity of CD9-containing vesicles. (*A*) Estimation of the fusion-facilitating ability of the vesicles in sperm–egg fusion. As shown in the experimental design, $CD9^{-/-}$ sperm were incubated with $CD9^{-/-}$ eggs (white circles) in media containing egg-released vesicles after the zona pellucida was removed from these eggs. CD9 was detected by anti-CD9 mAb conjugated with Alexa488. The eggs were preloaded with DAPI before incubation with the sperm, to allow counting of the number of fused sperm. (*Left*) $CD9^{-/-}$ eggs at 1 h after incubation with the sperm, as a negative control. *Center* $CD9^{-/-}$ eggs cultured in the medium containing CD9 collected from wild-type eggs. (*Right*) $CD9^{-/-}$ eggs cultured in the medium depleted of CD9 by beads conjugated with anti-CD9 mAb, showing the fused sperm to eggs (arrowhead), metaphase II–arrested chromosomes (*), a second polar body (open arrowhead), and CD9 translocated on the sperm heads (arrow). The fluorescent z-series images were projected as three-dimensional images. Scale bar: 20 μm. (*B*) Number of fused sperm with the zona-free eggs counted at 1 h after incubation (mean ± SEM): $CD9^{-/-}$ eggs as a negative control ($n = 51$), $CD9^{-/-}$ eggs cultured in the medium containing CD9 ($n = 112$), and $CD9^{-/-}$ eggs cultured in the medium depleted of CD9 by antibody-conjugated beads ($n = 74$). The total numbers of eggs examined are in parentheses. (*C*) Western blot analysis of the media incubated with $CD9^{+/+}$ eggs for CD9, HSP90, and HSP60. Loaded samples (left to right): The medium as a negative control, the medium containing the remnant material from 40 eggs per lane (bead-untreated and -treated), and 5 eggs per lane as a positive control. The albumin contained in the medium was detected by Coomassie brilliant blue staining as an internal control. The quantities of CD9 in the media were measured densitometrically (using National Institutes of Health Image software).

that the decreased amount of CD9 after the bead treatment was synchronized with that of a cytoplasmic chaperone, HSP90 (17), but not with a mitochondrial chaperone, HSP60 (18). Our analysis of the egg-conditioned medium indicated that CD9-containing vesicles contained HSP90, a conserved component of exosomes (9, 10).

To estimate the contribution of CD9-containing vesicles to sperm–egg fusion, we examined the restoration of the impaired sperm-fusing ability in $CD9^{-/-}$ eggs co-incubated with $CD9^{+/-}$ or $CD9^{+/+}$ eggs expressing endogenous CD9 (Figs. 5 and S4.4). We predicted that when sperm were incubated with a mixture of eggs, the vesicles released from $CD9^{+/-}$ or $CD9^{+/+}$ eggs would

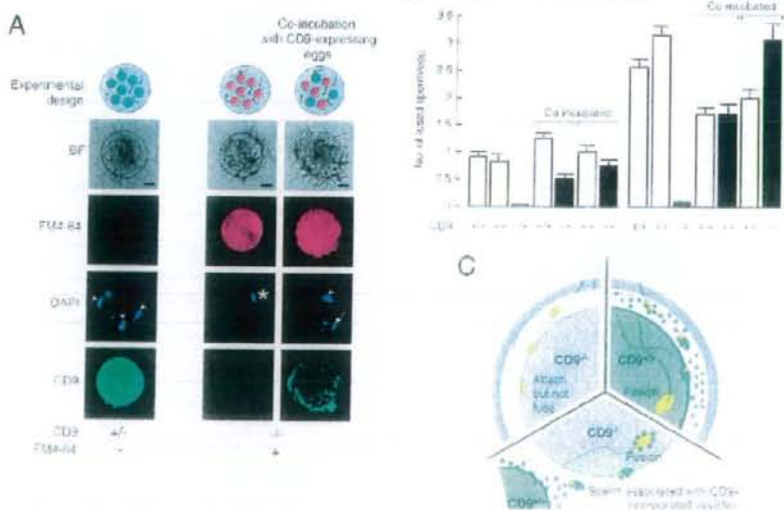

Fig. 5. Recovery of impaired fusion of $CD9^{-/-}$ eggs with sperm by CD9-containing vesicles. (*A*) Estimation of the fusion-facilitating ability of the vesicles in sperm–egg fusion. As shown in the experimental design, sperm were incubated with a mixture of CD9-expressing eggs (green circles) and $CD9^{-/-}$ eggs (red circles) after the zona pellucida was removed from these eggs. The eggs were preloaded with DAPI before incubation with sperm, to allow counting of the number of fused sperm. $CD9^{-/-}$ eggs were prestained with FM4–64 and thus were easily distinguished from CD9-expressing eggs after incubation with the sperm. (*Left*) $CD9^{+/-}$ eggs at 1 h after incubation with the sperm, as a positive control. (*Center*) $CD9^{-/-}$ eggs, as a negative control. (*Right*) $CD9^{-/-}$ eggs co-incubated with $CD9^{+/-}$ eggs, showing fused sperm to egg (arrowheads), metaphase II–arrested chromosomes (*), and extruded second polar body (arrow). The fluorescent z-series images were projected as three-dimensional images. CD9 was detected by anti-CD9 mAb conjugated with Alexa488. Scale bar: 20 μm. (*B*) Numbers of fused sperm with the zona-free eggs counted at 1 and 3 h after incubation (mean ± SEM). $CD9^{+/+}$ (1 h: $n = 34$; 3 h: $n = 55$), $CD9^{+/-}$ (1 h: $n = 71$; 3 h: $n = 79$), and $CD9^{-/-}$ eggs (1 h: $n = 100$; 3 h: $n = 115$) were separately incubated with sperm. Total number of coincubated eggs examined: $CD9^{+/-}$ eggs ($n = 54$) coincubated with $CD9^{-/-}$ eggs ($n = 60$), and $CD9^{+/-}$ eggs ($n = 65$) coincubated with $CD9^{-/-}$ eggs ($n = 74$) at 1 h; $CD9^{+/-}$ eggs ($n = 51$) coincubated with $CD9^{-/-}$ eggs ($n = 33$), and $CD9^{+/-}$ eggs ($n = 98$) coincubated with $CD9^{-/-}$ eggs ($n = 90$) at 3 h. (*C*) Schematic model of involvement of CD9-containing vesicles in sperm–egg fusion: $CD9^{+/-}$ (green), $CD9^{-/-}$ (light blue), and $CD9^{-/-}$ eggs coincubated with $CD9^{+/+}$ wild-type eggs with sperm (yellow).

interact with sperm, and these sperm could fuse with $CD9^{-/-}$ eggs. If sperm-fusing ability were regulated mainly by CD9-containing vesicles, then the number of sperm fused to $CD9^{-/-}$ eggs would be predicted to be almost equal to that fused to $CD9^{+/-}$ or $CD9^{+/+}$ eggs coincubated with $CD9^{-/-}$ eggs. We counted the number of fused sperm in coincubated CD9-expressing eggs ($CD9^{+/-}$ and $CD9^{+/+}$) and $CD9^{-/-}$ eggs. The $CD9^{-/-}$ eggs were prestained with FM4–64 (19), a fluorescent dye used to stain the membrane of live cells, and thus could be easily distinguished from the $CD9^{+/-}$ and $CD9^{+/+}$ eggs. FM4–64 did not transfer between the $CD9^{-/-}$ eggs and the $CD9^{+/-}$ or $CD9^{+/+}$ eggs. As shown in the experimental design, after the zona pellucida was removed from the eggs, $CD9^{-/-}$ eggs (red circles) were mixed with $CD9^{+/-}$ or $CD9^{+/+}$ eggs (green circles), and sperm were added to the medium containing these eggs (Fig. 5*A*). At 1 h after insemination, significant fusion of sperm with the $CD9^{-/-}$ eggs was facilitated (0.75 ± 0.11 and 0.50 ± 0.09 sperm fused per egg), corresponding to that in the $CD9^{+/-}$ (1.00 ± 0.13) and $CD9^{+/+}$ eggs (1.25 ± 0.10). At 3 h after insemination, the fusion of sperm with the $CD9^{-/-}$ eggs was restored (3.06 ± 0.30 and 1.70 ± 0.18 sperm fused per egg) to levels comparable to those in the $CD9^{+/-}$ (2.00 ± 0.15) and $CD9^{+/+}$ eggs (1.69 ± 0.13). We also detected a second polar body extruding from the $CD9^{-/-}$ eggs (Fig. 5*A Right*, arrow). In contrast, we did not observe the translocation of vesicles from the $CD9^{+/-}$ and $CD9^{+/+}$ eggs to the $CD9^{-/-}$ eggs when sperm were not added to the mixture, even after 10 h of incubation (Fig. S4*B*). These data demonstrate that the defect in the fusing ability of $CD9^{-/-}$ eggs is caused by dysfunction of the mechanism facilitating the sperm-fusing activity through CD9-containing vesicles.

To further study the involvement of CD9-containing vesicles in regulating sperm-fusing ability, we evaluated the capability of hamster eggs in sperm–egg fusion (Fig. S5). Hamster eggs have the ability to fuse with other mammalian sperm and thus are used as a tool to evaluate the fusing ability of human sperm (20). When hamster eggs were incubated with $CD9^{-/-}$ eggs after the zona pellucida was removed from these eggs, the sperm-fusing ability of these eggs was improved significantly. The sperm-fusing ability acquired through the exposure to hamster eggs was not as great as that produced by exposure to mouse eggs, probably due to the slightly different CD9 in hamster and mouse eggs (21). These results indicate that the function of CD9-containing vesicles in the acquisition of sperm-fusing ability is widely conserved in mammals.

Discussion

In sperm–egg fusion, there is a significant direct interaction between the cell membranes of sperm and eggs (1, 20, 22); however, our results demonstrate that CD9-containing vesicle–sperm interaction precedes the direct cell membrane interaction between sperm and eggs. Based on our data, we propose that the release of CD9-containing vesicles from eggs before fertilization facilitates the sperm-fusing ability that renders the sperm competent to fuse with $CD9^{-/-}$ eggs (Fig. 5*C*). Our finding of CD9-EGFP in living unfertilized eggs demonstrates that CD9-containing vesicles are present in the PVS, and that these vesicles accumulate inside the PVS during the germinal vesicle (1) and metaphase II-arrested stages (1). During this period, the egg undergoes drastic cytological changes with the increased number of microvilli (1, 22), predicting the correlation between vesicle release and microvilli formation. As expected, this correlation is supported by the finding that CD9 deficiency leads not only to impaired microvilli formation (8) (Fig. S2), but also to decreased accumulation of vesicles within the PVS. These data support the association between the release of CD9-containing vesicles from eggs and the formation of microvilli on the egg plasma membrane.

As reported previously, somatic cells are capable of releasing proteins and lipids included in membrane organelles, termed exosomes (9, 10), which are pinched out from the plasma membrane (23). Exosomes share many additional properties with retroviral particles, including similar lipid and protein compositions, such as tetraspanin (23). GM3 and HSP90 are known to be conserved components of exosomes (10). Our results show that CD9-containing vesicles released from eggs share these two components, implying that the vesicles are "exosome-like." Previous studies of macrophages have proposed that exosome biogenesis occurs only by outward budding at endosomal membranes, followed by the fusion of vesicle-laden endosomes with the plasma membrane (9, 23). If the CD9-containing vesicle were derived from exosomes and generated from the fusion of endosomes with the plasma membrane, then the vesicles would contain some proteases (9, 23), fuse with the sperm membrane, and possibly activate the sperm fusogenic factor(s) by enzymatic activities.

In hamster eggs, expansion of the PVS has been deemed essential or at least beneficial to normal fertilization (20, 21, 24), indicating that materials involved in fusion with sperm are released from eggs before fertilization in hamsters and in mice. Because anti-CD9 mAbs are not available for hamster CD9, we could not directly confirm CD9-containing vesicle release from hamster eggs before fertilization. Instead, our co-incubation assay demonstrated that hamster eggs facilitate the fusion of sperm with $CD9^{-/-}$ eggs, indicating that hamster eggs share a similar mechanism with mouse eggs through egg-released materials. Moreover, it has been reported that growing oocytes bind to sperm and transfer fluorescent dyes to the sperm head (25). At this stage, oocytes have CD9 on the cell membrane but lack CD9-containing vesicles (Fig. S1). We presume that the transfer of fluorescent dye from growing oocytes to sperm heads is mediated by CD9 on the cell membrane. Based on our findings, we propose that the CD9-containing vesicle has an ability to facilitate sperm—egg fusion. This knowledge has great potential for clinical applications, such as the induction of sperm–egg fusion using exogenous sources.

Materials and Methods

Animals. The mice that we produced were back-crossed into a C57BL/6 genetic background. Wild-type eggs were collected from C57BL/6 females (8–12 weeks old). Wild-type sperm were obtained from the epididymides of B6C3F1 males (8–12 weeks old). Hamster eggs were obtained commercially as frozen unfertilized eggs (NOSAN).

Antibodies and Chemicals. Antibodies against CD9 (KMC; BD PharMingen), beta-tubulin (Tub2.1; Sigma), HSP60 (24/HSP60; BD PharMingen), HSP90 (16F1; MBL), and GM3 (GMR6; Seikagaku) were used. Antibodies labeled with biotin by a labeling kit (Dojindo) and horseradish peroxidase-conjugated streptavidin (Sigma) were used for Western blot analysis. For immunostaining, antibodies were labeled directly with Alexa488 and Alexa546 using labeling kits (Invitrogen). FM4–64 (Invitrogen) was used to define the lipid bilayer of live eggs without disturbing sperm–egg fusion (10 μM at final concentration). We used DAPI (Invitrogen), a fluorescent dye that slowly permeates the living cell membrane (semipermeable) and slowly leaks out of cells after washing relative to Hoechst33342 (permeable), in counting the number of sperm fused per egg.

Transgenic Mice. The construct expressing mouse CD9 tagged at the N terminus with EGFP (CD9-EGFP) was subcloned into plasmid DNA-containing mouse ZP3 promoter (26). The expression cassette was excised by restriction enzyme digestion and microinjected into fertilized eggs of C57BL/6 mice, according to standard techniques (27).

Genotyping and RT-PCR. Mouse genotyping and RT-PCR were performed following standard procedures (27). (Primer sets are listed in Table S1).

Egg Collection. Eggs were collected from the oviduct 14–16 h after human chorionic gonadotropin injection (4). The eggs were placed in a drop of TYH

medium (28). Sperm collected from the epididymides were capacitated in a 100-μl drop of medium. The eggs were incubated with 1.5×10^5 sperm/ml at 37°C in 5% CO_2, and unbound sperm were washed away. The zona pellucida was removed from the eggs with acidic Tyrode's solution (4) or a piezo manipulator (11). A hole was punched through the zona pellucida with a piezo manipulator, and the eggs were removed. All materials were aspirated, including the medium but not the eggs, and used as "remnants."

Immunostaining. Zona-intact live eggs were stained with diluted antibodies in TYH medium for 30 min at 37°C, and the nonspecifically accumulated antibodies in the PVS were washed away after a brief incubation (30 min) in the medium. To measure the fluorescent intensities of GM3, three types of eggs were stained by Alexa546-labeled anti-GM3 mAb in TYH medium for 30 min, then washed in the medium for 30 min. Staining was visualized using a laser scanning confocal microscope (LSM 510 META; Carl Zeiss).

Electron-Microscopic Analysis. Live eggs were incubated with anti-CD9 mAb and anti-rat IgG mAb tagged with 5-nm gold beads. After incubation, the eggs were fixed by glutaraldehyde and osmic acid solutions. Ultra-thin sections were prepared as described in ref. 29. Eggs denuded with acid Tyrode's solution were fixed with a mixture of paraformaldehyde and glutaraldehyde and osmic acid solutions.

***In Vitro* Fertilization.** To observe the fusion with the sperm, zona-intact and zona-free eggs were incubated with DAPI (10 μg/ml) in the medium for 20 min, then washed before the sperm were added. This procedure allowed the staining of only fused sperm nuclei by dye-transfer into sperm after membrane fusion. At 1 h or 3 h after incubation in a 30-μl drop of medium, the eggs were fixed with a mixture of paraformaldehyde and glutaraldehyde for 20 min at 4°C.

Monitoring the Association of CD9-Containing Vesicles with Sperm. Eggs collected from $Tg^+CD9^{-/-}$ females were set in a 30-μl drop of TYM medium. The sperm were added to the eggs at a final concentration of 1.5×10^5/ml after incubation in the medium for 2 h. Posts of latex beads were deposited around the eggs. A glass coverslip was carefully pressed down onto the posts until the egg were fixed. The medium containing eggs and sperm was cooled to 10°C before observation. Cooling reduced the sperm motility. This procedure allowed us to measure the CD9-EGFP fluorescence on the sperm head using a confocal microscope. Images of the sperm were captured at 1 frame/s. The average value of the fluorescent intensities of CD9-EGFP at 0 s was set to 100%, and the final concentration of antibodies was adjusted to 50 μg/ml. The data are measurements of serial images from 15 wild-type sperm in triplicate dishes.

Collection of CD9-Containing Vesicles. The medium containing the vesicles was collected from denuded wild-type eggs. The eggs were cultured in a 60-μl drop of medium for 2 h after the zona pellucida was removed from the eggs. Collecting the medium containing the vesicles required an incubation time of 2 h. The collected medium was used for analysis of vesicle components and evaluation of sperm-fusing ability. CD9-depleted medium was used as a negative control. After the zona pellucida was removed from $CD9^{-/-}$ eggs, the eggs were incubated with the sperm in the medium containing CD9-incorporated vesicles for 1 h, for comparison with the vesicle-depleted medium. Details are shown in Fig. S3.

Western Blot Analysis. Quantities of proteins were examined by Western blot analysis, as described in ref. 4. As an internal loading control, quantities of albumin included in the medium were examined using Coomassie brilliant blue staining. Details are shown in Fig. S3.

Coincubation of Two Types of Eggs. $CD9^{-/-}$ eggs and CD9-expressing eggs ($CD9^{+/-}$ and $CD9^{+/+}$) were incubated in each 30-μl drop of medium after the zona pellucida was removed from these eggs. At 2 h after incubation, the $CD9^{-/-}$ eggs were added into the cultured medium of the CD9-expressing eggs. Sperm were added into the medium containing two types of eggs and incubated for 1 or 3 h. Details are shown in Fig. S4A. The frozen hamster eggs also were incubated with the $CD9^{-/-}$ eggs and wild-type sperm for 1 h. The zona pellucida of frozen hamster eggs was hardened, and removing the zona pellucida using acid Tyrode's solution took 5 min. Details are shown in Fig. S5A.

ACKNOWLEDGMENTS. This work was supported by a Precursory Research for Embryonic Science and Technology (PRESTO) grant from the Japanese Ministry of Health, Labor and Welfare and by a Grant-in-Aid for Scientific Research from the Japanese Ministry of Education, Culture, Sports, and Technology.

1. Yanagimachi R (1994) in *The Physiology of Reproduction*, eds Knobil E, Neill JD (Raven, New York), pp 189–317.
2. Kaji K, *et al.* (2000) The gamete fusion process is defective in eggs of Cd9-deficient mice. *Nat Genet* 24:279–282.
3. Le Naour F, Rubinstein E, Jasmin C, Prenant M, Boucheix C (2000) Severely reduced female fertility in CD9-deficient mice. *Science* 287:319–321.
4. Miyado K, *et al.* (2000) Requirement of CD9 on the egg plasma membrane for fertilization. *Science* 287:321–324.
5. Hemler ME (2003) Tetraspanin proteins mediate cellular penetration, invasion, and fusion events and define a novel type of membrane microdomain. *Annu Rev Cell Dev Biol* 19:397–422.
6. Barraud-Lange V, Naud-Barriant N, Bomsel M, Wolf J-P, Ziyyat A (2007) Transfer of oocyte membrane fragments to fertilizing spermatozoa. *FASEB J* 21:3446–3449.
7. Joly E, Hudrisier D (2003) What is trogocytosis and what is its purpose? *Nat Immunol* 4:815.
8. Runge K-E, *et al.* (2007) Oocyte CD9 is enriched on the microvillar membrane and required for normal microvillar shape and distribution. *Dev Biol* 304:317–325.
9. Trajkovic K, *et al.* (2008) Ceramide triggers budding of exosome vesicles into multivesicular endosomes. *Science* 319:1244–1247.
10. Wubbolts R, *et al.* (2003) Proteomic and biochemical analyses of human B cell-derived exosomes: Potential implications for their function and multivesicular body formation. *J Biol Chem* 278:10963–10972.
11. Yamagata K, *et al.* (2002) Sperm from the calmegin-deficient mouse have normal abilities for binding and fusion to the egg plasma membrane. *Dev Biol* 250:348–357.
12. Mitsuzuka K, Handa K, Satoh M, Arai Y, Hakomori S (2005) A specific microdomain ("glycosynapse 3") controls phenotypic conversion and reversion of bladder cancer cells through GM3-mediated interaction of alpha3beta1 integrin with CD9. *J Biol Chem* 280:35545–35553.
13. Yamashita T, *et al.* (2003) Enhanced insulin sensitivity in mice lacking ganglioside GM3. *Proc Natl Acad Sci USA* 100:3445–3449.
14. Kotani M, Ozawa H, Kawashima I, Ando S, Tai T (1992) Generation of one set of monoclonal antibodies specific for a-pathway ganglio-series gangliosides. *Biochim Biophys Acta* 1117:97–103.
15. Chen MS, *et al.* (1999) Role of the integrin-associated protein CD9 in binding between sperm ADAM 2 and the egg integrin alpha6beta1: Implications for murine fertilization. *Proc Natl Acad Sci USA* 96:11830–11835.
16. Miller B-J, Georges-Labouesse E, Primakoff P, Myles D-G (2000) Normal fertilization occurs with eggs lacking the integrin alpha6beta1 and is CD9-dependent. *J Cell Biol* 149:1289–1296.
17. Callahan M-K, Garg M, Srivastava P-K (2008) Heat-shock protein 90 associates with N-terminal extended peptides and is required for direct and indirect antigen presentation. *Proc Natl Acad Sci USA* 105:1662–1667.
18. Cheng M-Y, Hartl F-U, Horwich A-L (1990) The mitochondrial chaperonin hsp60 is required for its own assembly. *Nature* 348:455–458.
19. Bolte S, *et al.* (2004) FM-dyes as experimental probes for dissecting vesicle trafficking in living plant cells. *J Microsc* 214:159–173.
20. Yanagimachi R, Yanagimachi H, Rogers B-J (1976) The use of zona-free animal ova as a test system for the assessment of the fertilizing capacity of human spermatozoa. *Biol Reprod* 15:471–476.
21. Ponce R-H, Yanagimachi R, Urch U-A, Yamagata T, Ito M (1993) Retention of hamster oolemma fusibility with spermatozoa after various enzyme treatments: A search for the molecules involved in sperm–egg fusion. *Zygote* 1:163–171.
22. Primakoff P, Myles D-G (2002) Penetration, adhesion, and fusion in mammalian sperm–egg interaction. *Science* 296:2183–2185.
23. Booth A-M, *et al.* (2006) Exosomes and HIV Gag bud from endosome-like domains of the T cell plasma membrane. *J Cell Biol* 172:923–935.
24. Okada A, Yanagimachi R, Yanagimachi H (1986) Development of a cortical granule-free area of cortex and the perivitelline space in the hamster oocyte during maturation and following ovulation. *J Submicrosc Cytol* 18:233–247.
25. Zuccotti M, Yanagimachi R, Yanagimachi H (1991) The ability of hamster oolemma to fuse with spermatozoa: Its acquisition during oogenesis and loss after fertilization. *Development* 112:143–152.
26. Rankin T-L, *et al.* (1998) Human ZP3 restores fertility in Zp3 null mice without affecting order-specific sperm binding. *Development* 125:2415–2424.
27. Hogan B, Costantini F, Lacy E (1986) in *Manipulating the Mouse Embryo* (Cold Spring Harbor Lab Press, Cold Spring Harbor, NY), pp 217–252.
28. Toyoda Y, Chang M-C (1974) Capacitation of epididymal spermatozoa in a medium with high K-Na ratio and cyclic AMP for the fertilization of rat eggs in vitro. *J Reprod Fertil* 36:125–134.
29. Toshimori K, Saxena D-K, Tanii I, Yoshinaga K (1998) An MN9 antigenic molecule, equatorin, is required for successful sperm–oocyte fusion in mice. *Biol Reprod* 59:22–29.

Human Sclera Maintains Common Characteristics with Cartilage throughout Evolution

Yuko Seko[1,2], Noriyuki Azuma[2], Yoriko Takahashi[1], Hatsune Makino[1], Toshiyuki Morito[3], Takeshi Muneta[3], Kenji Matsumoto[4], Hirohisa Saito[4], Ichiro Sekiya[5], Akihiro Umezawa[1*]

1 Department of Reproductive Biology and Pathology, National Institute for Child and Health Development, Tokyo, Japan, 2 Department of Ophthalmology, National Center for Child Health and Development, Tokyo, Japan, 3 Section of Orthopaedic Surgery, Tokyo Medical and Dental University, Tokyo, Japan, 4 Department of Allergy and Immunology, National Institute for Child and Health Development, Tokyo, Japan, 5 Section of Cartilage Regeneration, Tokyo Medical and Dental University, Tokyo, Japan

Abstract

Background: The sclera maintains and protects the eye ball, which receives visual inputs. Although the sclera does not contribute significantly to visual perception, scleral diseases such as refractory scleritis, scleral perforation and pathological myopia are considered incurable or difficult to cure. The aim of this study is to identify characteristics of the human sclera as one of the connective tissues derived from the neural crest and mesoderm.

Methodology/Principal Findings: We have demonstrated microarray data of cultured human infant scleral cells. Hierarchical clustering was performed to group scleral cells and other mesenchymal cells into subcategories. Hierarchical clustering analysis showed similarity between scleral cells and auricular cartilage-derived cells. Cultured micromasses of scleral cells exposed to TGF-βs and BMP2 produced an abundant matrix. The expression of cartilage-associated genes, such as Indian hedge hog, type X collagen, and MMP13, was up-regulated within 3 weeks in vitro. These results suggest that human 'sclera'-derived cells can be considered chondrocytes when cultured ex vivo.

Conclusions/Significance: Our present study shows a chondrogenic potential of human sclera. Interestingly, the sclera of certain vertebrates, such as birds and fish, is composed of hyaline cartilage. Although the human sclera is not a cartilaginous tissue, the human sclera maintains chondrogenic potential throughout evolution. In addition, our findings directly explain an enigma that the sclera and the joint cartilage are common targets of inflammatory cells in rheumatic arthritis. The present global gene expression database will contribute to the clarification of the pathogenesis of developmental diseases such as high myopia.

Citation: Seko Y, Azuma N, Takahashi Y, Makino H, Morito T, et al. (2008) Human Sclera Maintains Common Characteristics with Cartilage throughout Evolution. PLoS ONE 3(11): e3709. doi:10.1371/journal.pone.0003709

Editor: Che John Connon, University of Reading, United Kingdom

Received July 31, 2008; **Accepted** October 8, 2008; **Published** November 12, 2008

Copyright: © 2008 Seko et al. This is an open-access article distributed under the terms of the Creative Commons Attribution License, which permits unrestricted use, distribution, and reproduction in any medium, provided the original author and source are credited.

Funding: This study was supported by Research Fellowships of the Japan Society for the Promotion of Science (JSPS) for Young Scientists; a grant from the Ministry of Education, Culture, Sports, Science and Technology (MEXT) of Japan and Health and Labor Sciences Research Grants; by a Research grant on Health Science Focusing on Drug Innovation from the Japan Health Science Foundation; by the Program for Promotion of Fundamental Studies in Health Science of the Pharmaceuticals and Medical Devices Agency; by a grant from the Terumo Life Science Foundation; by a Research Grant for Cardiovascular Disease from the Ministry of Health, Labor and Welfare; and by a Grant for Child Health and Development from the Ministry of Health, Labor and Welfare.

Competing Interests: The authors have declared that no competing interests exist.

* E-mail: umezawa@1985.jukuin.keio.ac.jp

Introduction

The eye receives information from the outside as the retinal image, converting it into electrical signals for the brain, leading to visual perception. The retinal image is stabilized by the balance of intraocular pressure and the curvatures of the scleral and corneal envelope. In order to keep this balance, the rigidity of the sclera and the cornea are essential, especially the sclera must be rigid enough for the eyeball to be rotated by powerful extraocular muscles adhering to the sclera. The sclera and the corneal stroma that are anatomically continuous have common characteristics such as mechanical rigidity, and share a common origin, i.e., the neural crest. However, the cornea and the sclera are different in transparency: the cornea is completely transparent to produce a sharp image on the retina; the sclera is opaque to avoid the internal light scattering affecting the retinal image. This corneal transparency has been attributed to significant changes in the structure, especially of collagen fibrils, in the latter stages of development [1]. Multipotent progenitor/precursor cells of corneal stroma are identified from the mouse eye [2]. On the other hand, existence of multipotent progenitor/precursor cells in the sclera remains unclarified. Although the sclera does not contribute significantly to visual perception, scleral diseases such as refractory scleritis, scleral perforation and pathological myopia are considered incurable or difficult to cure.

Microarray analysis of murine scleral development [3] and global sequencing analysis from the human scleral cDNA library [4] have been reported. To clarify pathogenesis of developmental diseases such as high myopia, a database of genes expressed in the sclera of younger donors is important. We here demonstrate with a global expression database of human infant sclera that the sclera derived from the neural crest evolutionarily retains characteristics of cartilage.

Results

Isolation and cell culture of human scleral cells

Scleral tissues were excised from surgical specimens collected during treatment for retinoblastoma. The scleral tissue was cut into smaller pieces and cultured in the growth medium. The scleral cells began growing out almost one week after the start of cultivation. Scleral cells exhibited a fibroblast-like spindle shape or polygonal shape in morphology when cultured in monolayer (Fig. 1A). The cells from PD 5 to PD 31 rapidly proliferated in culture, and propagated continuously (Fig. 1B). The cells stopped replicating and became broad and flat at PD 43 or 264 days, indicating that they had entered senescence. The morphological changes are PD-dependent.

Global outlook by hierarchical clustering and PCA

To clarify the specific gene expression profile of scleral cells, we compared the expression levels of 54,675 probes in the cultured scleral cells and other cultured cells (Table 1) using the Affymetrix GeneChip oligonucleotide arrays. We first performed hierarchical clustering and PCA on the expression pattern. PCA showed similarity between scleral cells and chondrocytes derived from elastic cartilage (Fig. 2A). Hierarchical clustering analysis based on all probes showed similarity between scleral cells and chondrocytes (Fig. 2B). This similarity led us to hypothesize that the scleral cells are chondrocytes when proliferated ex vivo, or have a chondrogenic potential. We then performed PCA from the expression data of cartilage-associated genes, including aggrecan, Sox9, and parathyroid hormone receptor (Table S1). These genes are categorized as "cartilage condensation" or "proteoglycan biosynthesis" according to Gene Ontology. PCA based on cartilage-associated genes demonstrated that scleral cells are grouped into the same category that includes chondrocytes, synovial cells, and synovial fluid-derived cells (Fig. 2C). The synovial cells and synovial fluid-derived cells used in this study have a strong chondrogenic potential [5–7]. Hierarchical clustering analysis based on the cartilage-associated genes also demonstrated that sclera, cartilage, synovium, and joint fluid are categorized into the same group (Fig. 2D, Fig. 2E, Fig. S1).

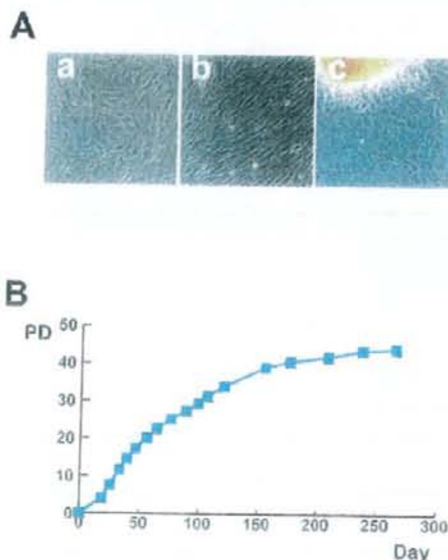

Figure 1. Proliferation of human 'sclera'-derived cells. A. Photograph of primary cultured human 'sclera'-derived cells by phase-contrast microscope. **B.** Growth curve of cultured human 'sclera'-derived cells. Vertical axis indicates population doublings (PD) and horizontal axis indicates days after innoculation of human 'sclera'-derived cells.
doi:10.1371/journal.pone.0003709.g001

Table 1. Human cells analyzed in this study.

Title	Description
Bone marrow	Bone marrow-derived cell (P1)
Hepatocyte	Hepatocyte (P0)
Endometrium	Endometrial cell
Synovium	Synovium-derived cell (P1)
Joint fluid	Joint fluid-derived cell (P1)
Muscle	Muscle-derived cell (P1)
Bone	Cancellous bone-derived cell (P1)
Fat	Subcutaneus fat-derived cell (P1)
Amniotic epithelium	Amniotic epithelial cell (P4)
Umbilical cord (1)	Umbilical cord-derived cell (P0) (1)
Umbilical cord (2)	Umbilical cord-derived cell (P0) (2)
Cartilage	Auricular cartilage-derived cell (P1)
Sclera	Sclera-derived cell (P1)
Cornea (stroma)	Keratocyte (P1)
Periostium	Periostium-derived cell (P1)
Dermis	Dermal fibroblast (P2)
Cortical bone	Cortical bone-derived cell (P3)

Gene chip analysis was performed using RNAs from the cells obtained from each tissue. The cells obtained from bone marrow, liver, synovium, joint fluid, muscle, bone, and fat were cultivated as previously described [31–33]. Amniotic epithelial cells and umbilical cord-derived cells were cultured after each tissue was manually separated from the placenta and minced by surgical knife and scissors. Auricular cartilage-derived cells, periostium-derived cells, dermal fibroblasts, and cortical bone-derived cells started to be cultured after each tissue was manually separated from surgical specimens from patients with polydactyly or microtia. Keratocytes and scleral cells were obtained from corneal stroma and sclera (also see the Materials and Methods section). "Endometrium" was obtained from the homogenized endometrial cells under liquid nitrogen. All cells were harvested under signed informed consent, with the approval of the Ethics Committee of the National Institute for Child and Health Development, Tokyo. Signed informed consent was obtained from donors and the surgical specimens were irreversibly de-identified. All experiments handling human cells and tissues were performed in line with the Tenets of the Declaration of Helsinki. Global gene expression profiles of those cells are uploaded to GEO accession #GSE10934 at http://www.ncbi.nlm.nih.gov/geo/index.cgi.
P: passage. P0 and P1 represents primary cell culture and cell culture one passage after starting primary culture from tissues, respectively.
doi:10.1371/journal.pone.0003709.t001

Chondrogenesis of human scleral cells

After reaching 70–80% sub-confluence, we started the micromass culture of scleral cells. Four weeks after culture in a chondrogenic medium containg TGF-β1 and BMP2, a pellet of human scleral cells exhibited a spherical shape (Fig. 3A). This pellet showed an alcian blue positive extracellular matrix, indicating that cultured micromasses of scleral cells exposed to TGF-β1 and BMP2 produce an abundant matrix (Fig. 3B). RT-PCR analysis demonstrated that scleral cells at passage 0 expressed aggrecan, COL2A, SOX5, SOX6, SOX9, and PTHR1 mRNAs

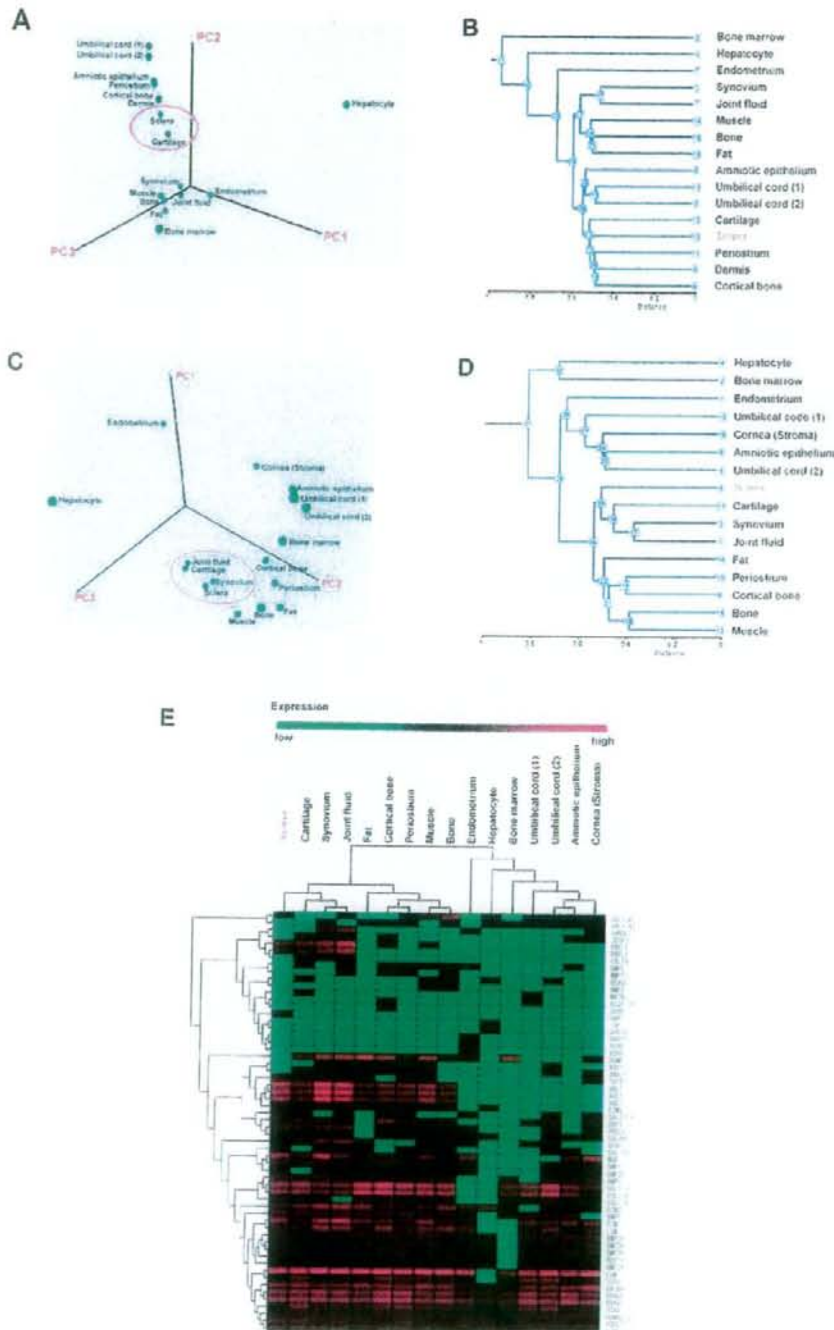

Figure 2. Global gene expression analysis of cultured human cells. A. Three-dimensional representation of PCA of gene expression levels (Human Genome U133 Plus 2.0: 54,675 probes). The gene expression data from scleral cells following one passage from the primary cultured cells (equivalent to appropriately 4 PDs) were used for PCA. Sclera and cartilage are positioned closely adjacent (shown in circle). **B.** Hierarchical clustering

analysis based on the expression of all genes (Human Genome U133 Plus 2.0: 54,675 probes, NIA Array Analysis) shows similarity between scleral cells and chondrocytes. **C.** PCA of the cartilage-associated gene expression (Table S1). Sclera, cartilage, synovium, and joint fluid are positioned closely adjacent (shown in circle). **D.** Hierarchical clustering analysis based on expression levels of the cartilage-associated genes (NIA Array Analysis). Sclera, cartilage, synovium, and joint fluid are categorized into the same group. **E.** Hierarchical clustering analysis (TIGR MeV, see the Materials & Methods) with the heat map, based on expression levels of the cartilage-associated genes. Each row represents a gene; each column represents a cell population. Sclera, cartilage, synovium, and joint fluid are categorized into the same group. Cells derived from cartilage, synovium, and joint fluid are capable of generating cartilage in vivo [7,34].
doi:10.1371/journal.pone.0003709.g002

(Fig. 3C). These expressions were maintained in the cells after 10 population doublings. After in vitro chondrogenesis of scleral cells, COL10A, SOX5, IHH, and MMP13 mRNA expressions increased. After human scleral cells labeled with DiI were implanted into a rat cartilage defect, the cells expressed type II collagen (Fig. 3D). These results demonstrated that human scleral cells retained chondrogenic potential both in vitro and in vivo.

Discussion

Tracing back of human scleral cells to chondrocytes through cultivation

This study was undertaken to investigate if human sclera has a chondrogenic nature like chicken sclera [8,9]. Bioinformatics of human scleral cells suggest similarity between scleral cells and

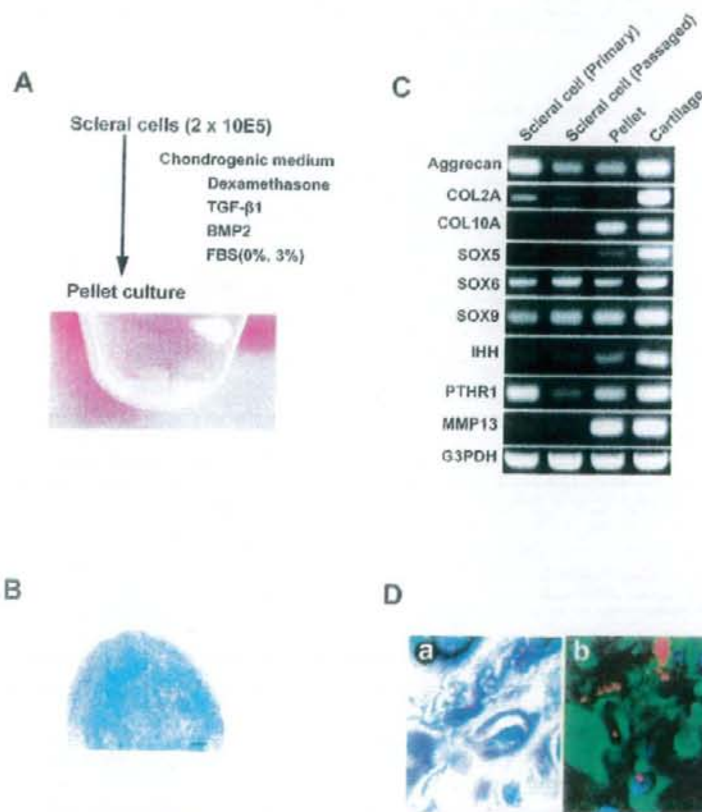

Figure 3. Chondrogenesis of human 'sclera'-derived cells. A. In vitro chondrogenesis. 'Sclera'-derived cells were centrifuged to make a pellet and cultured in chondrogenic medium for 4 weeks. Macroscopic feature is shown. **B.** Histological section of a pellet by micromass culture in a chondrogenic medium stained with alcian blue. Bar: 100 µm. **C.** Reverse transcriptase-PCR for cartilage-associated genes. Total RNAs were prepared from scleral cells at passage 0, at 10 population doublings, after in vitro chondrogenic induction, and normal cartilage as a positive control. **D.** Histological sections 4 weeks after transplantation of human scleral cells into cartilage defect of the knee in a rat. (a) Toluidin blue staining. (b) Immunohistochemistry. Human scleral cells were labeled with DiI (red). Nuclei were stained with DAPI (blue). Type II collagen was shown as green.
doi:10.1371/journal.pone.0003709.g003

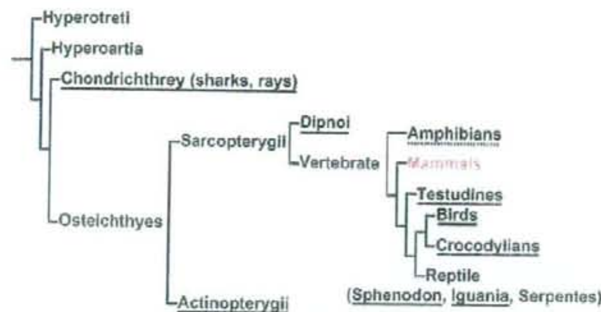

Figure 4

Figure 4. The distribution of scleral cartilage in vertebrates. The chondrogenic nature of the sclera is conserved across species. The figure is modified from Franz-Odendaal, TA, et al., 2006 [10]. Species that have cartilage in the sclera are underlined; species with either absence or presence of cartilage in the sclera, depending on family, are dot-underlined; species without cartilage in the sclera are non-underlined.
doi:10.1371/journal.pone.0003709.g004

chondrocytes, and this similarity may be attributed to evolution of the sclera (Fig. 4), that is, animals such as elasmobranch, teleost fish, amphibians, reptiles and birds incorporate the development of a cup of hyaline cartilage in the sclera [10]. Scleral cartilage is hypothesized to counter against the traction force of the extraocular muscle and against the accommodative force to move or deform the lens by intraocular muscles. In this paper, we employ the global gene expression approach to human scleral cells. As a result, scleral cells and chondrocytes are found to share common chondrogenic characteristics.

Simulation of chondrogenic process during development

The phenotype of the differentiated chondrocyte is characterized by the synthesis, deposition, and maintenance of cartilage-specific extracellular matrix molecules, including type II collagen and aggrecan [11–13]. Three-dimensional culture is a prerequisite for exhibition of this chondrogenic phenotype in vitro since the phenotype of differentiated chondrocytes is unstable in culture and is rapidly lost during serial monolayer subculturing [14–16]. The expression pattern of cartilage-associated genes in sclera-derived cells after induction is consistent with that of chondrocytes during development (Fig. 3C, Fig. S2): a) Consistent expression of type II collagen and aggrecan, markers of early-phase chondrogenesis [17,18] in sclera-derived cells, indicates that sclera-derived cells retain their chondrogenic nature as a default state; b) Induction of type X collagen and MMP13 genes after pellet formation of sclera-derived cells may simulate late-stage chondrogenesis. In addition, other chondrocyte-associated genes, such as sox5, IHH, and PTHR1 were also up-regulated. Sox5 functions as a transcription factor necessary for chondrogenesis [19,20]. IHH promotes chondrogenesis as a cytokine [21], and PTHR1 mediates parathyroid hormone signaling as a specific receptor [18]. These results suggest that ex vivo culture of sclera-derived cells simulates the developmental process of chondrogenesis. Despite the chondrogenic nature of sclera-derived cells, lack of cartilage in the sclera in humans may be attributed to cis- and trans-regulation of cartilage-associated gene(s), or an unclarified inhibitory mechanism that was altered during evolution (Fig. 4).

Implication of chondrogenic nature of sclera in diseases

The fact that the gene expression pattern of the human fibrous sclera is similar to that of cartilage is interesting not only as comparative anatomy but also from a patho-etiological view point. The sclera and the joint cartilage are common targets for inflammatory cells in rheumatic arthritis [22,23] or polychondritis [24], implying common proteins between the sclera and the synovium. Although the target protein(s) remains unclarified, our findings directly explain an enigma that both the sclera and the joint cartilage are affected in rheumatic arthritis. Furthermore, mutations in genes for type II and type XI collagen are a cause of Stickler syndrome [25,26]. Patients with Stickler syndrome have joint deformity and severe high myopia due to an abnormality of the sclera. These affected lesions may be attributed to the chondrogenic nature of human sclera. In conclusion, our present study shows a chondrogenic potential of human sclera and explains the etiology of scleral disorders, at least in part. In addition, we would like to emphasize that the first database of gene expression in the human infant sclera (uploaded to GEO accession #GSE10934 at http://www.ncbi.nlm.nih.gov/geo/index.cgi) may contribute to the elucidation of scleral diseases in the future.

Materials and Methods

Isolation and cell culture of human scleral cells

Scleral tissues were excised from surgical specimens as a therapy of retinoblastoma, under signed informed consent, with the approval (approval number, #156) of the Ethics Committee of the National Institute for Child and Health Development, Tokyo. Signed informed consent was obtained from donors, and the surgical specimens were irreversibly de-identified. All experiments handling human cells and tissues were performed in line with the Tenets of the Declaration of Helsinki. The scleral pieces were cut into smaller pieces and cultured in the growth medium (GM): Dulbecco's modified Eagle's medium (DMEM)/Nutrient mixture F12 (1:1) with high glucose supplemented with 10% fetal bovine serum, insulin-transferrin-selenium, and MEM-NEAA (GIBCO).

Oligonucleotide microarray

Total RNAs were isolated from cultured scleral cells in the growth medium without any induction of differentiation to perform the gene chip analysis. Total RNA was extracted from a total of 3×10^6 cultured human scleral cells and other mesenchymal cells (Table 1) using RNeasy Plus mini-kit® (Qiagen, Maryland, USA) according to